Physical vulnerability curve construction and quantitative risk assessment of a typhoon-triggered debris flow via numerical simulation: A case study of Zhejiang Province, SE China

Tengfei Wang[1,5], Kunlong Yin[1], Yuanyao Li[2], Lixia Chen[3], Changgui Xiao[4], Haomeng Zhu[4], Cees van Westen[5]

1. Faculty of Engineering, China University of Geosciences, Wuhan, 430074, China

2. Institute of Geological Survey, China University of Geosciences, Wuhan, 430074, China

3.Institute of Geophysics and Geomatics, China University of Geosciences, Wuhan, 430074, China

4. Institute of Geology of Zhejiang Province, Hangzhou, 310007, China

5. Faculty of Geo-Information Science and Earth observation, University of Twente, the Netherlands

Corresponding author: Yuanyao Li, email: liyuanyao@cug.edu.cn

Abstract: Typhoons are recurrent meteorological phenomena in the South-eastern coastal area of China. They often trigger debris flows and other types of slope failure which cause significant economic damage and loss of life in an area with dense population and high economic activities. Accurate prediction of Typhoon-triggered debris flows and determination of the potential risk zones are crucial for risk management. However, little effort has been devoted to risk assessment by constructing the physical vulnerability curves in the typhoon-affected area. To cope with this deficiency, this paper presented a quantitative method to build up the physical vulnerability curves of buildings by modeling the debris flow intensity and building damage features. In this study, the Wangzhuangwu (WZW) watershed was selected, which was impacted by a debris flow induced by Typhoon Lekima on 10 August 2019. At first, detailed field investigation and interpretation of remote sensing imagery were carried out to analyze the geological characteristics, mechanism of the debris flow, and construct a database of building damage features. The 2019 debris flow initiation, movement and deposition processes were modelled based on the Soil Conservation Service-curve number (SCS-CN) approach and a two-dimensional finite model (FLO-2D). The reconstructed debris flow depth and extend were validated with observed information. Then, we proposed physical vulnerability curves for different type of building structures by combining the damage degree of buildings and the modelled debris flow intensity (flow depth and impact pressure). Based on the validated rheological parameters, the potential intensity of future debris flows was modelled considering different recurrence frequency of the triggering rainfall. Finally, the vulnerability index and economic risk of buildings to debris flow events with different frequencies were calculated using different vulnerability functions. The uncertainty of quantitative risk assessment was considered in the intensity indictor and building structure. The RC (reinforced concrete) frame building has stronger resistance than the non-RC frame building under same intensity of debris flow, and the vulnerability function using the impact pressure as the intensity indictor is more conservative than which using the flow depth. The proposed approach efficiently generated the physical vulnerability curves and debris flow risk map that can be used for effective disaster prevention in debris flow-prone areas.

Keywords: Typhoon-triggered debris flow; Physical vulnerability curve; Numerical simulation;

Quantitative risk assessment

1. Introduction

Debris flows pose a frequent and devastating geological hazard in mountainous areas causing a significant threat to human life, property, and infrastructure (Tang et al., 2009; Ouyang et al., 2019). The south-eastern coast of China is particularly affected by debris flows due to heavy rainfall caused by typhoons (Zhao et al., 2018; Zhang et al., 2021). On August 10th, 2019, Super typhoon Lekima produced extremely concentrated rainfall in the northern part of Zhejiang province, triggering numerous debris flows causing significant loss of life and property damage(Nie et al. 2021; Zhou et al. 2022; Liang et al. 2022).

Quantitative risk assessment of debris flows is a crucial tool for disaster prevention and town planning(Eidsvig et al. 2014; Zhang et al. 2015a; Bout et al. 2018).It involves evaluating the potential hazards associated with debris flows, identifying the elements at risk (such as buildings, people, and critical infrastructure) that could be affected by a debris flow event, and assessing the vulnerability of these area and population to those hazards. The assessment process typically involves analyzing historical data, modeling potential hazards and impacts, and using this information to inform decision-making and planning efforts to mitigate the risk of debris flows (Eidsvig et al. 2014).

Hazard assessment of debris flows is based on simulation of the dynamic processes (Luna et al. 2012; Bout et al. 2018), which allows to calculate various indicators that describe the characteristics of debris flows. The analysis of the dynamic processes of debris flows is essential for assessing hazard and risk zones(Guo et al. 2020; Figueroa-García et al. 2021). This requires a good understanding of the properties and characteristics of debris flows, such as formation mechanisms, frequency, and intensity(Chang et al. 2020; He et al. 2022). Numerical simulation using physical models can quantitatively analyze the movement of debris flows(van Asch et al. 2014; Zhang et al. 2018; Horton et al. 2019). One popular model for this is the FLO-2D model, a depth-integrated continuum method that has been used since the 1990s (O'Brien et al. 1993). Researchers have used the FLO-2D model to analyze the dynamic movement of debris flows in earthquake-affected areas and to clarify the formation conditions and movement processes of mine waste debris flows (Zou et al. 2016a; Chang et al. 2020; Tang et al. 2022). However, the validity of the model is heavily dependent on the basal friction model and the parameter values used, so validation based on site investigations is necessary, especially in extreme debris flow cases(Chen et al. 2019). Additionally, the model doesn't include the hydrological process, so a suitable hydrological model to calculate peak discharge and runoff processes of debris flows is crucial for the reliability of prediction results(Zhang et al. 2015a).

Vulnerability assessment is a challenging aspect of debris flow risk assessment(Fuchs et al. 2007; Jaiswal and van Westen 2013; Ciurean et al. 2017). The value of vulnerability is closely linked to the intensity of the debris flow and the damage index of the elements at risk. The methods of debris flow vulnerability assessment have evolved from qualitative to quantitative (Li et al., 2010; Peduto et al., 2017). However, the quantitative vulnerability assessment also faces some uncertainty. For example, the vulnerability of buildings has a high uncertainty with respect to the lack of extensive damage database of buildings damaged by debris flows, the varying characteristics of debris flows, and specific building characteristics (number of floors, opening of buildings, protection by other objects). Vulnerability of people inside buildings depends on the damage degree of the building, and the number of floors. Vulnerability of people outside buildings depends on the warning time, and escape possibilities. The primary focus of vulnerability assessment is on buildings, which plays a vital role in the vulnerability assessment, since it’s indicative of the overall damage, and closely linked to population vulnerability.

Physical vulnerability curve based on the statistics method has been seen an effective method in quantitative vulnerability assessments, which could relate the intensity of the debris flow to the damage index of elements at risk. The construction of physical vulnerability curve requires intensity information of debris flows and damage information of elements at risk. Due to the difficulty of monitoring dynamic parameters along debris flow paths and the infrequency of past event records providing information on debris flow intensity, the dynamic numerical model was gradually employed to reconstruct the debris flow process and establish the hazard intensity(Zhang et al. 2018; Horton et al. 2019). The selection of indictors that express the impact of debris flows play a vital role in vulnerability curve construction. Several methods have been proposed to describe the impact of debris flows on elements at risk based on the calculated indicators from dynamic processes such as the flow depth and velocity (Cui et al. 2011; Papathoma-Köhle et al. 2012; Quan Luna et al. 2013; Kang and Kim 2016). Tang et al. (1993) and Fangqiang et al. (2006) proposed the use of maximum flow depth and maximum flow velocity, respectively, as the intensity indicators (Tang et al. 1993; Fangqiang et al. 2006). Hu and Ding (2012) suggested the use of maximum momentum, as a kinetic energy factor, to more directly express the impact force(Hu and Ding 2012). Jakob et al. (2012) and Ouyang et al. (2019) proposed the two-factor classification method that combines maximum depth and maximum momentum is more effective in reflecting the destruction caused by debris flows than single-factor of maximum momentum (Jakob et al. 2012; Ouyang et al. 2019). However, comparing to these indicators above, the impact pressure could express the damage capability of debris flows to buildings more essentially from statics and dynamic aspects(Quan Luna et al. 2011; Kang and Kim 2016).

In this paper, a numerical model was used to reconstruct the catastrophic debris flows induced by super Typhoon Lekima, which occurred on August 10th 2019 in Linan district, Zhejiang province, and to predict future risk under different recurrence periods. We conducted a detailed site investigation based on field measurements and UAV-based remote sensing to obtain the digital elevation model (DEM) and digital orthophoto model (DOM) of the debris flow. A numerical calculation was then performed by integrating the hydrologic model (SCS-CN) and the FLO-2D model to reconstruct the debris flow for the typhoon event. A series of vulnerability curves for RC frame and non-RC frame buildings were constructed using the flow depth and impact pressure as the intensity indictors. The vulnerability and risk values of the buildings under different rainfall recurrence periods were predicted by considering the debris flow intensity, vulnerability, and economic value of buildings. The quantitative risk assessment approach proposed in this paper may provide guidance for the mitigating the risk of debris flows.

2. Study area

2.1 Topography and engineering geological conditions

The Wangzhuangwu watershed locates in Linan District of Zhejiang Province, China, upstream of Daoshi town (Fig.1). The main rock outcrops in the area are Cambrian limestone and argillaceous limestone, which are overlaid by Quaternary deposits including silty clay and gravel. These geological conditions make the area susceptible to slope erosion and undercutting, which provide a source of material for debris flows. The study area was affected by Typhoon Lekima, which caused 81 debris flows, one of which was the Wangzhuangwu (WZW) debris flow, which damaged 109 houses, interrupted roads, and resulted in a direct economic loss of about 4 million RMB (US $ 57,554).

2.2 Climate characteristics and rainfall conditions

The study area is in a subtropical monsoon climate zone with four distinct seasons and high average annual rainfall of 1613.9mm, with an average of 158 days of rain per year. Most of the rainfall occurs between April and October, with an average of 1173.5mm (Fig.2a). The rainstorms associated with monsoon troughs occurring from April to early July, are widespread and have low intensity; while typhoon rainstorms, occur from mid-July to September, and very intensive and last for a short time. In the case of Typhoon Lekima, the daily precipitation reached 252.2mm on August 10th, 2019, as recorded by a rain gauge in Wangzhuangwu Village (Fig.2b).

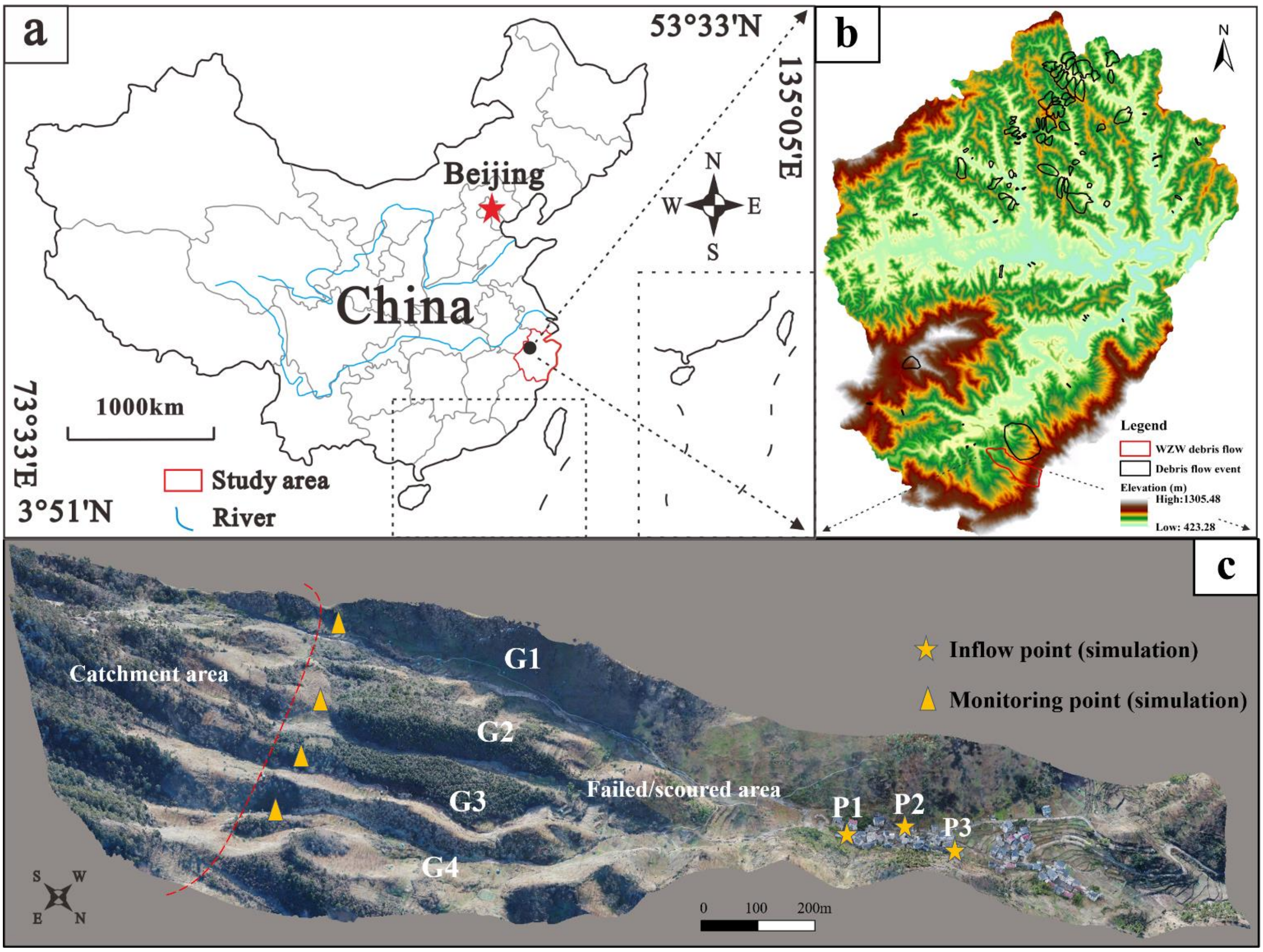

Figure 1 Location and three-dimensional model of the Wangzhuangwu (WZW) watershed: (a) Location of the WZW gully in Zhejiang Province, China; (b) Regional setting and debris flow distribution of Daoshi town; (c) Three-dimensional model of WZW watershed established by UAV, four main gullies (G1-G4), three monitoring points (P1-P3), catchment area and sourced area (splited by the red line)

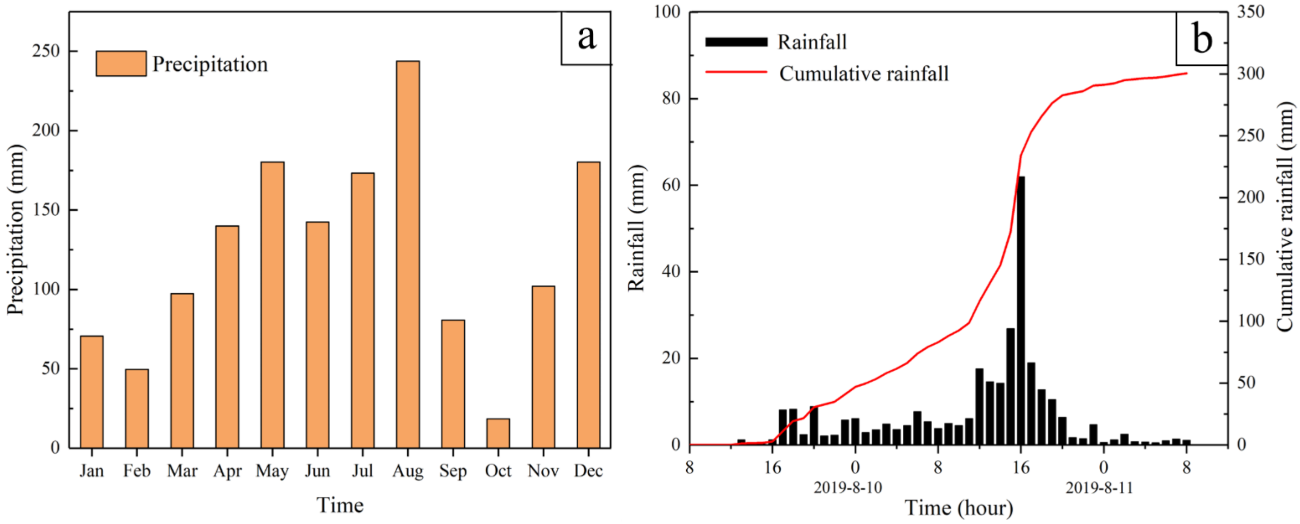

Figure 2 Monthly rainfall of the study area and hourly rainfall during Typhoon Lekima: (a) Distribution of monthly rainfall in the study area in 2018; (b) Hourly and cumulative rainfall during the Typhoon Lekima in August 2019

3. Methodology

The methodological procedure of the study can be divided into three steps (Fig.3). In the first step, we investigated the physical characteristics of the 2019 WZW debris flow through field work and aerial imaging. On this basis, we reconstructed the run-out process and calculated the intensity parameters such as flow depth and flow velocity using a numerical model. In the second step, we constructed the vulnerability curves and functions of buildings with different structures using the intensity indictors of the reconstructed debris flow and the damage information of buildings. Then we calculated the vulnerability index of buildings in future scenario based on the validated rheological parameters and the vulnerability functions. In the third step, we predicted the debris flow risk under different recurrence intervals using the results from the first and second steps. This methodology allows for a detailed analysis of the debris flow event and the potential risk to buildings in the area under different recurrence intervals, helping to inform disaster management and mitigation strategies.

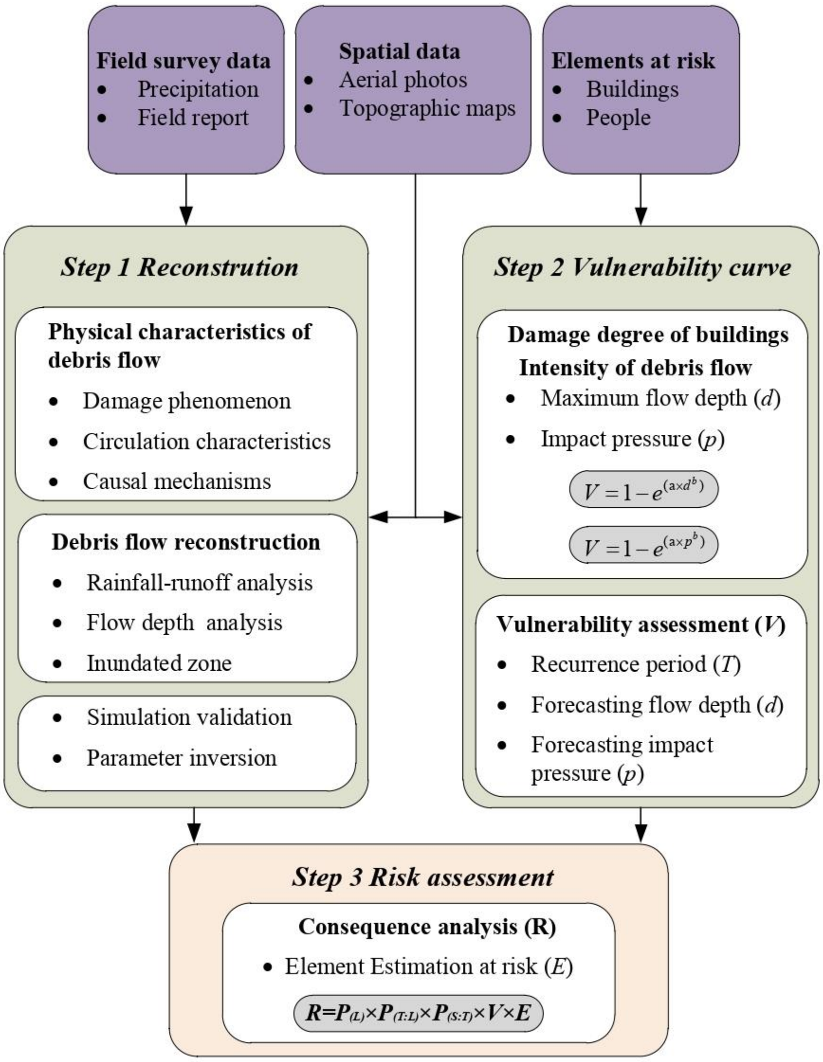

Figure 3 Flowchart of the methodology applied in this study

3.1 Field investigation

In the study, field investigation mainly consists of two components:

(1) Obtaining field measurements and topographic data. This includes conducting a photogrammetric survey using unmanned aerial vehicles (UAVs) to acquire topographic information of the study area (Fig.4a). DJI Phantom 4 and Mavic Pro drones were used flying at a height of 100 meters above the ground and take photographs with an 80% lateral and transversal overlap (Fig.4a). The aerial images were then used to create a 3D model and a digital elevation model (DEM) of the study area with help of the Context Capture (Fig.1c). This information was used to model the debris flow and identify geomorphic features such as the development of valleys, water catchment areas, ground undulation degree, slope ratio, and vegetation.

(2) Sampling evidences of the debris flow activity, to understand its characteristics such as flow depth, velocity, and sediment size (Fig.4b~d). The vegetation affected in the movement path of the debris flow and the buildings were mapped, evidence of damage such as scars and mud traces were collected and stored in a database with basic features of the buildings such as construction structure, material, number of floors. Damage characteristics were also recorded such as the damage degree, the impact azimuth angle, and the height of the impact. The damage degree was determined using a classification scheme proposed by Kang and Kim (2016)(Kang and Kim 2016). The disaster database includes information on 212 buildings, of which 109 were affected by the 2019 WZW debris flow.

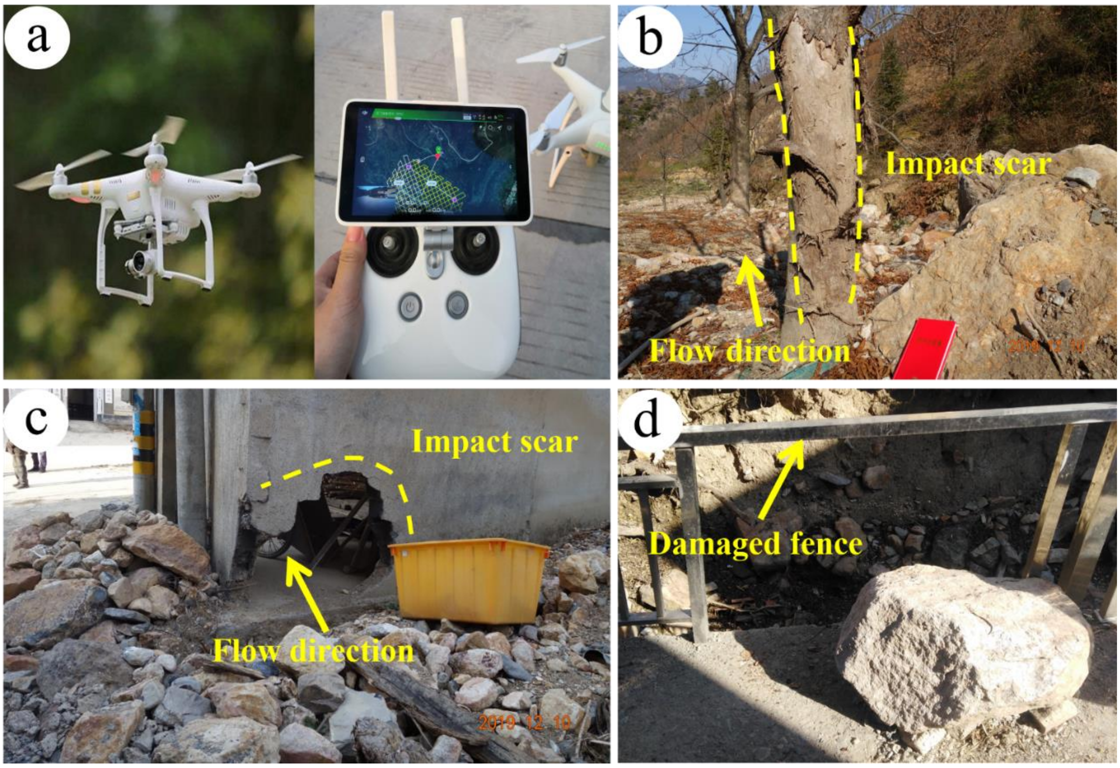

Figure 4 Fieldwork methods and sampling evidence of the 2019 WZW debris flow activity: (a) Photogrammetric survey using UAV; (b) Impact scar of the trees in the movement path of the debris flow; (c) Impact scar of the buildings in the influence area of the debris flow; (d) A fence damaged by the debris flow

The particle size distribution of the debris flow was also investigated for determining the debris flow density, which can be calculated using the formula below(Yu et al. 2013):

$$\gamma_D = \gamma_0 + \gamma_V P_2 (P_{0.05})^{0.35} \tag{1}$$

Where γ_D is the average density of the 2019 WZW debris flow (g/cm^3); γ_V is the minimum density of a viscous debris flow (2.0 g/cm^3); γ_0 is the minimum density of a debris flow (1.5 g/cm^3); P_2 is the percentage of coarse particles with the diameter more than 2 mm, and $P_{0.05}$ is the percentage of fine particles with the diameter less than 0.05 mm.

3.2 Dynamic simulation of the debris flow

The dynamic simulation of the debris flow can be divided into two parts. The initial stage involved simulating the rainfall in the region to generate a discharge hydrograph and assess the impact of rainfall intensity on the flow. The subsequent stage consisted of simulating the debris flow, which integrated the outcomes of the rainfall and entrained material models. In this process, we use a series of validation methods for the validation of model results and selection of parameters.

3.2.1 Hydrological analysis

The HEC-HMS software was utilized to calculate the rainfall-runoff process of the WZW debris flow. This software is based on the concept of semi-distributed modeling and is widely used in hydrology (HEC-HMS 2010). The SCS-CN method, one of the most widely accepted hydrologic methods in HEC-HMS to estimate runoff, taking into account the indirect impact of human activities(Laouacheria and Mansouri 2015). The direct runoff Q (mm) is calculated using the following equation:

$$Q = \begin{cases} \dfrac{(P-0.2S)^2}{(P+0.8S)} & P \geq 0.2S \\ 0 & P < 0.2S \end{cases} \tag{2}$$

Where P (mm) is the precipitation; S (mm) is the potential maximum infiltration which is related to soil texture, land use, and AMCs. The potential maximum infiltration, S, is determined by the following equation:

$$S = \frac{25,400}{CN} - 254 \tag{3}$$

Where SCS curve number (CN) is an index that reflects the combination of hydrologic soil group, land treatment classes, and prior moisture conditions. It can be determined by referencing the standard table provided by SCS-USA and finding the matching soil description.

The precipitation (mm) for various rainfall recurrence periods was calculated using the Gumbel distribution. The cumulative distribution function of the Gumbel distribution is represented as follows(Matti et al. 2016):

$$F_X(x) = \exp\left\{-\exp\left[-\frac{x-\xi}{\alpha}\right]\right\} \tag{4}$$

where X is a random variable, x is a possible value of X, ξ is the location parameter calculated using $\mu_X = \xi + 0.5772\alpha$ and α is the scale parameter calculated using $\sigma^2 = \pi^2\alpha^2/6$, where μ_X and σ^2 are the mean and variance of the data set, respectively.

The daily rainfall intensity for different recurrence periods of 20, 50, and 100 years were calculated using the Gumbel distribution method based on historical rainfall data from 1971 to 2018 in the study area (Fig.5a). The resulting intensities were 245.51 mm/day for 20-year, 293.16 mm/day for 50-year, and 328.87 mm/day for 100-year recurrence period. The rainfall intensity under 20-year recurrence is roughly the same with that during Typhoon Lekima, so the simulation results of debris flow under Typhoon Lekima can be considered representative of that under 20-year recurrence period. The hydrographs of the catchment area of G1 gully were derived by using the precipitation as input to the SCS-CN hydrologic method in HEC-HMS software, and the results were illustrated in Figure 5b.

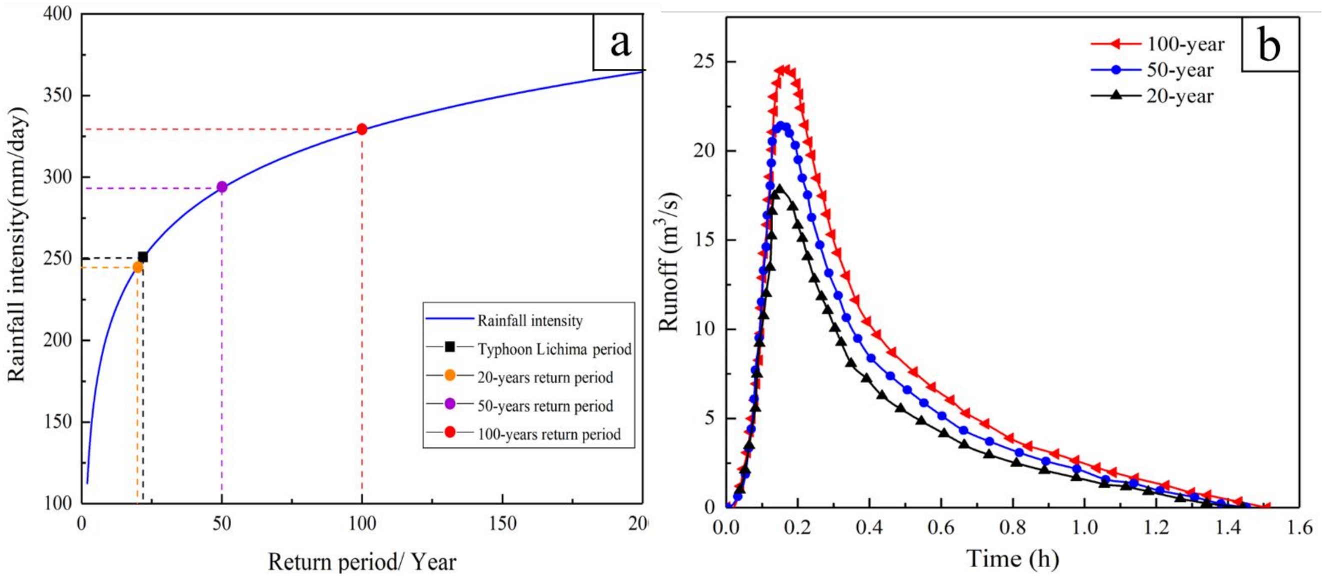

Figure 5 Daily rainfall intensity and flow hydrographs of G1 gully under different recurrence periods: (a) Daily rainfall intensity under Typhoon Lichima and three recurrence periods; (b) Flow hydrographs of G1 gully under three recurrence periods

3.2.2 Runout analysis

The FLO-2D model is a two-dimensional debris flow evolution model that was used to simulates the runout process and quantifies metrics of the WZW debris flow. The simulation process is implemented through numerical integration of motion equations and fluid volume conservation(O'Brien et al. 1993). FLO-2D model uses a Eulalia formulation with a finite difference numerical scheme that requires an input hydrograph as a boundary condition. A quadratic rheological model is employed in FLO-2D, which considers the Bingham shear stress as a function of sediment concentration. The model also considers a combination of turbulent and dispersive stress components that depend on a modified Manning *n* value:

$$S_f = \frac{\tau_y}{\gamma_m h} + \frac{K\eta v}{8\gamma_m h^2} + \frac{{n_{td}}^2 v^2}{h^{4/3}} \tag{5}$$

where S_f is the total friction slope; τ_y is the yield stress (Pa); γ_m is the specific gravity of the fluid matrix; h is the flow depth (m); K is the laminar flow resistance; η is the dynamic viscosity (Pa·s); v is the flow velocity (m/s); n_{td} is an empirically modified Manning n value of the mixture; n, η and τ_y are expressed as follow:

$$n = 0.33_{v}^{-0.15}\exp(C_{v}^{-0.15})\ln h \tag{6}$$

$$\eta = \alpha_1 e^{\beta_1 C_v} \tag{7}$$

$$\tau_y = \alpha_2 e^{\beta_2 C_v} \tag{8}$$

Where C_v is volume concentration, which represents the discharge relation between water flow and debris flow. α_1, α_2, β_1, β_2 are empirical coefficients.

In our study, the SCS-CN model hydrological analysis was used to obtain the surface runoff discharge, which serves as a boundary condition for the FLO-2D model. This model simulates the movement process and intensity coefficients such as flow depth (h) and flow velocity (v).

3.2.3 Model calibration and validation

A series of rheological parameters needed to be defined in FLO-2D software simulation process. These parameters include the Manning's roughness coefficient (n), flow resistance parameter (K), sediment concentration (C_v), and empirical coefficients (α, β). Since there are no independent estimates of the model's friction parameters, the initial rheological parameters are determined based on previous studies, physical experiments, and field investigations (Liu and Lei 2003; Chang et al. 2017). The model calibration is then carried out through trial-and-error selection and adjustment of the input rheological parameters. The goal of the calibration process is to adjust the parameters until the simulated and observed characteristics of the debris flow show a good consistency.

The methodology for validating the accuracy of the reconstruction result of the 2019 WZW debris flow involves overlaying the reconstructed influence area (A1) obtained from the FLO-2D model with the actual influence area observed during the investigation period(Scheidl and Rickenmann 2009). Figure 6 shows the schematic diagram of the methodology. The evaluation parameter (τ and ∂) is used to express the overall accuracy of the reconstruction result and is calculated using the equations:

$$\tau = \frac{S_X}{S_{observed}} - \frac{S_Y}{S_{observed}} - \frac{S_Z}{S_{observed}} + \frac{V_X}{V_{observed}} \tag{9}$$

$$\partial = \frac{\tau + 2}{4} \tag{10}$$

where S_X is the positive accuracy area; S_Y is the negative accuracy area; S_Z is the missing accuracy area; $S_{observed}$ is the actual influence area; V_X is the correct reconstruction volume, while $V_{observed}$ is the actual influence volume. The range of τ is between -2 and 2. Here we propose a normalized value, ∂, to express the standard accuracy, which is between 0 and 1, respectively on behalf of no overlap and perfect overlap.

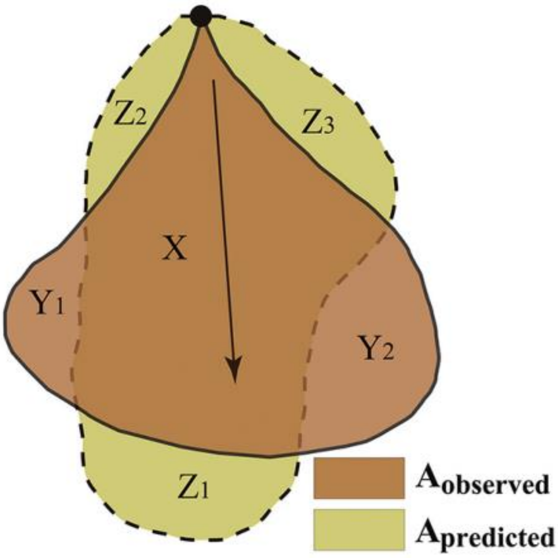

Figure 6 Schematic diagram of reconstruction result verification(Chen et al. 2021)

In addition to overlaying the reconstructed and actual influence areas, the accuracy of the reconstruction result of the 2019 WZW debris flow is also evaluated by setting three monitoring points (P1-P3) at the positions of observation buildings (Fig.1c). The variation of flow depth in the simulation process is monitored at these points, and the maximum flow depth of the debris flow at the monitoring points is compared to the height of mud marks left on the same buildings. This provides an additional perspective for evaluating the accuracy of the reconstruction result.

3.3 Risk assessment

Debris flow risk is analyzed based on the classic definition of risk, which is the product of the probability of a debris flow event occurring, the vulnerability of elements exposed to the event, and the potential losses(Fell et al. 2008; Corominas et al. 2013). The focus is on the risk to buildings from debris flow, and the risk is calculated using the following equation:

$$R=P_{(L)}\times P_{(T:L)}\times P_{(S:T)}\times V\times E \quad (11)$$

Where R represents the annual total risk of buildings. $P_{(L)}$ is the probability of a debris flow event, which is countdown of the recurrence period. $P_{(T:L)}$ is the probability of a debris flow reaching a specific point, which can be determined from the output of numerical simulation. For the elements located in the inundation zone, the $P_{(T:L)}$ is 1. $P_{(S:T)}$ is the probability of elements at a certain point during a debris flow event. For the static building, the $P_{(S:T)}$ is 1. V and E represent the vulnerability index and the economic value of the element at risk.

3.3.1 Hazard assessment

The debris flow hazard represents the potential for damage at a specific location under a certain condition. It is primarily determined by the temporal probability of that condition occurring and the intensity of the debris flow. In this study, the temporal probality is the countdown of the recurrence periods. The debris flow intensity is a measure of the destructive capability of the debris flow which includes the siltation capability and the impact capability. The siltation capability can be reflected by the accumulative depth, while the impact capability can be reflected by the impact pressure(Ouyang et al. 2019). The impact pressure of the debris flow consisits of the dynamic overpressure and hydrostastic pressure. These forces depend on the peak discharge, velocity, volume, and grain-size distribution of debris flow(Zanchetta et al. 2004). The dynamic overpressure and the hydrostatic pressure can be used to reflect the impact capability:

$$P = (1/2)\rho gh + \rho v^2 \quad (12)$$

Where ρ is the debris flow density (kg/m^3), h is the depth of the debris flow (m), g is the gravity acceleration (m/s^2), v is the velocity of the debris flow (m/s). The first term in Eq.12, $(1/2)\rho gh$ represents the mean hydrostatic pressure component. The second term, ρv^2, is the dynamic overpressure component.

3.3.2 Vulnerability estimation

Vulnerability is a concept that is defined differently by scientists with various backgrounds. In the field of engineering geology, vulnerability is defined as the "degree of loss" of a given element exposed to a debris flow. It ranges from 0 (no loss) to 1 (total loss). The availability of intensity and damage information of the WZW debris flow makes it a significant case study. Furthermore, the range of building damage provides an opportunity to evaluate vulnerability using a function that links the debris flow intensity to the extent of damage.

In our approach, we utilized the buildings damage data obtained from field investigation in combination with information from modelling outputs to calculate vulnerability functions. This method facilitates the computation of vulnerability functions based on both debris flow accumulation height and impact pressure.

A comprehensive analysis of field survey data, photographs, and reports is conducted to determine building damage. To evaluate the damage caused by debris flows, a damage classification system was implemented, which includes complete destruction, extensive damage, moderate damage, and slight damage categories. In the inundation area, the degree of building damage is determined by evaluating the damage to the exterior walls, the presence of cracks in the walls, loss of external and internal wall components, internal room flooding, or damage to the main building column.

4. Results

4.1 Characteristics and damage of the 2019 WZW debris flow

Remote sensing interpretation and field investigation were used to survey the disaster features and describe the mechanism of the WZW debris flow caused by the Typhoon Lekima. The catchment area is 1.55 km^2, with an elevation that ranges from 606 m to 1178 m above sea level, and a gentle slope of 15° from southeast to northwest. The study area consists of four main gullies (G1-G4) that converge about 50 m upstream of the village (Fig.1c and Fig.7a). The channelized debris flow is characterized by a long travel distance, a large volume of transported material, and a high level of destructiveness. The formation area of the debris flow is 0.28 km^2, characterized by steep terrain, poor vegetation cover, and loose soil on the valley slopes. Soil erosion and shallow landslides frequently occur during heavy rainfall, providing a source of loose soil and debris that accumulate in the gully, leading to the formation of the debris flow (Fig.7c). Additionally, the channels in the initiation area are steep and straight, giving the debris flow a high entrainment capacity (Fig.7b).

The accumulation area of the debris flow occurred at the exit of a residential area, resulting in the accumulation of mud and sand in the form of a depositional fan (Fig.7d). The grain-size characteristics of the matrix in the debris fan were analyzed using the sieving method from two locations (S1 and S2) with a 2×2 m rectangular windows (Fig.8). The density of the debris flow (γ_D) was determined based on the particle-size distribution of samples taken from different locations on the fan according to Eq.1.

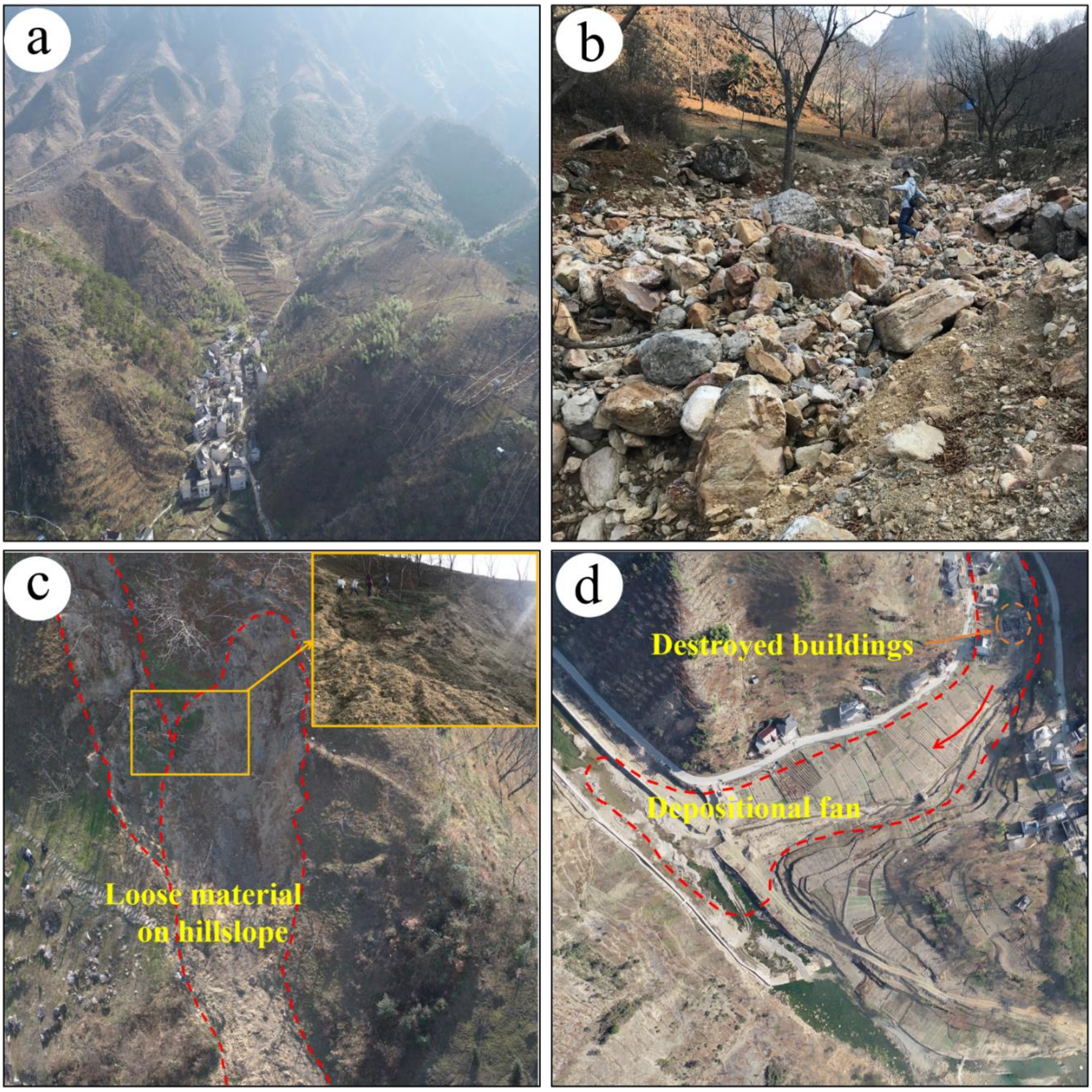

Figure 7 Overview of the debris flow: (a) Topography of the catchment area; (b),(c) A large amount of loose material on hillslopes and in the channels which provided abundant material sources for the WZW debris flow; (d) Location of the deposition fan and destroyed buildings after the debris flow.

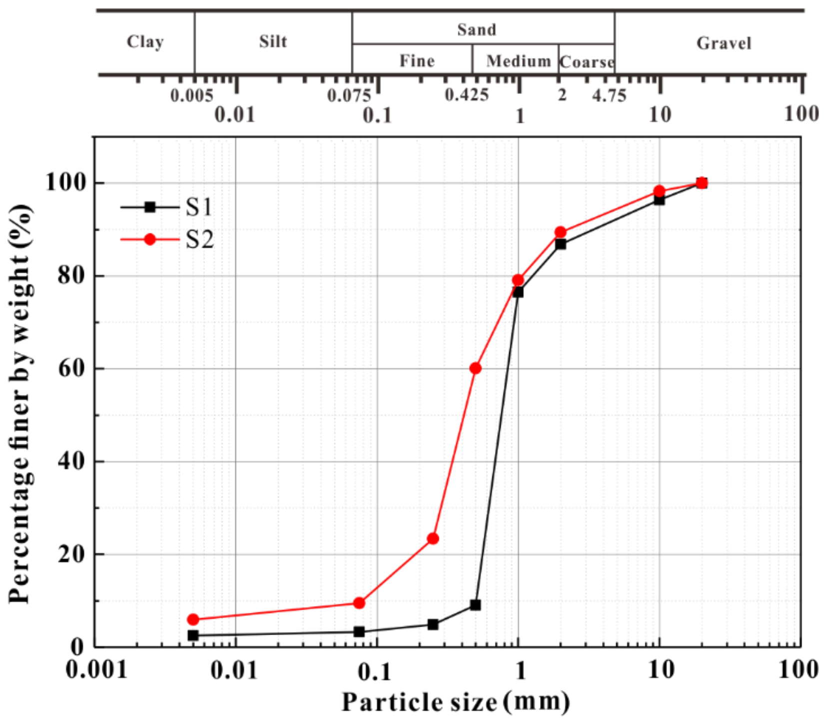

Figure 8 Particle gradation of the 2019 WZW debris flow deposits

The basic features of buildings in the Wangzhuangwu village were investigated. A total of 211 items were classified according to the structural type, number of floors, and order of impacted by debris flows (Tab.2). In this work, buildings are classified into two structural types: reinforced-concrete (RC) frame and non-concrete (non-RC) frame. In which, the non-RC frame mainly includes masonry, wooden frame. For the same intensity of the debris flow (such as impact pressure and flow depth), the buildings with RC frame have higher resistance than those with non- RC frame. Most buildings in the area have one or more than three floors. Combining the flow paths of the 2019 WZW debris flow and the location of the buildings, we classified these buildings into three orders to be impacted by debris flows. More than 80% buildings located in the first order to be impacted, which means they will face greater influence of debris flows compared to others.

The 2019 WZW debris flow, comprising of mud, sand, and rocks swept through the WZW village which is situated in the path of the debris flow, causing damage to buildings including residential houses and public facilities. 109 of the total 211 buildings were damaged with different degrees, and the number of these damaged buildings with different features was shown in Table 2. Based on the classification criteria mentioned in section 3.3.2, these damaged buildings were classified into four categories (Tab.3). Figure 9 illustrates some examples of buildings in different damage categories.

Table 2 Building features and damaged number distribution

Building feature	Building feature classes	Number of buildings	Number of buildings damaged
Structural type	Reinforced-concrete frame	130	68
	Non-concrete frame	81	41
Number of floors	⩾3	85	44
	2	40	22

	1	86	43
Order of impacted	First	171	94
	Second	30	9
	Third	10	6

Table 3 Damage classification scheme for the buildings

Damage degree	Damage description	Vulnerability index (used value)	Number of buildings Non-RC frame	RC frame
Slight	Slight non-structural damage, stability not affected, damage to furnishings or fittings	0.1-0.3 (0.2)	16	47
Moderate	Cracks in the wall, stability unaffected, flooding of the internal rooms and damage to the furnishing	0.3-0.6 (0.45)	14	13
Extensive	Partly destroyed, loss of parts of external and internal walls, evacuation necessary, reconstruction of destroyed parts	0.6-0.8 (0.7)	4	8
Complete	Totally destroyed, evacuation necessary, complete reconstruction	0.8-1.0 (1.0)	7	0

Figure 9 Buildings in different degrees damaged by 2019 WZW debris flow: (a) Slight damage; (b) Moderate damage; (c) Extensive damage; (d) Complete damage

4.2 Reconstruction of the 2019 WZW debris flow

The 2019 WZW debris flow run-out process was reconstructed using FLO-2D software, with a 2m grid model obtained from a photogrammetric survey using UAV as the DEM. The flow hydrograph, triggered by rainfall during the typhoon Lekima period, was calculated using the SCS-CN hydrologic method and HEC-HMS software. The inflow points were set at four locations (Q1-Q4) corresponding to the catchment areas of G1-G4, with a duration (T) of 1.5h, which matched the actual duration of the 2019 WZW debris flow.

The optimized simulation result of the 2019 WZW debris flow shows a high degree of agreement with actual measurements from the field investigation. The accuracy was evaluated by comparing the reconstructed influence area (A1) obtained from the FLO-2D software with the actual influence area observed during the field investigation period, using equation 9, 10 and the parameters in Table 4. The standard evaluation parameter, ∂, which expresses the overall accuracy of the simulation result, reached

0.902, indicating that the optimized simulation result matches well with the actual 2019 WZW debris flow.

The maximum flow depth at points P1-P3 in the debris flow path also matches well with the height of the mud marks left on buildings observed during the field investigation. The flow depth evolution process is shown in Figure 10. When the debris flow occurs, sediment reaches the locations of P1 and P2 successively, and the flow depth rises rapidly to the maximum in 0.4h. Since P1 and P2 are in the upper part of the circulation zone, the sediment has a certain capacity for circulation and entrainment. The flow depth curve shows a slight downward trend after reaching the maximum and then maintains a steady state until the end of the debris flow. As P3 is in the lower part of the circulation zone, the circulation and entrainment capacity of the debris flow have a certain degree of reduction, and the flow depth curve tends to stabilize after the rapid rise.

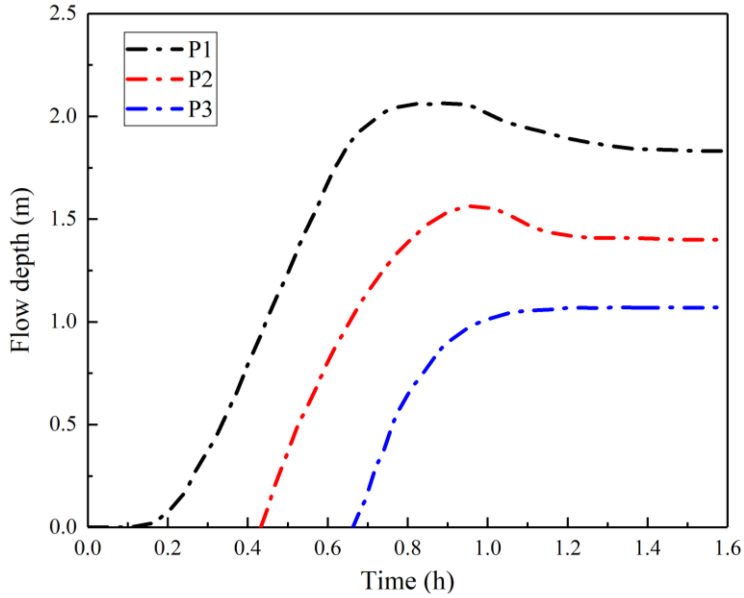

Figure 10 Flow depth evolution process over time at the point of P1~P3 in the debris flow path

The optimized simulation result has been calibrated to maintain a high degree of consistency with the actual situation through the methods described above. The optimized rheological parameters required for the simulation are presented in Table 5. These can be used in the simulation of debris flow under rainfall conditions of different recurrence periods.

Table 4 Validation parameters and results of numerical simulation accuracy

Parameter	Unit/10^3m^2				Unit/10^4m^3						
	A_X	A_Y	A_Z	$A_{observed}$	V_X	$V_{observed}$	α	β	γ	δ	τ
Value	15.66	2.35	1.53	18.02	1.46	1.53	0.87	0.13	0.08	0.96	1.61

Table 5 The rheological parameters for WZW debris flow simulation

Parameters		Value
Manning's roughness coefficient (n)		0.2
Flow resistance parameter (K)		4782
Sediment concentration (Cv)		0.48
Empirical coefficients	α1	0.0765
	β1	16.9
	α2	0.0648
	β2	6.2

The optimized simulation results obtained by FLO-2D software including the flow velocity and the flow depth are shown in Figure 11. The study simulated an area affected by the debris flow of approximately 1.86×105 m^2. Most of the affected area had a flow depth of less than 2 m, with 53.96% of the inundation area having a flow depth less than 1 m, 46% having a flow depth between 1 and 2 m, and only 0.04% having a flow depth greater than 2 m. The area with relatively high flow depth was concentrated at the mouth of a gulley in the entrance of a village.

The flow velocity in the inundation area is mainly below 2m/s, with 48.9% and 49.5% of the area having flow velocity less than 1m/s and 1-2m/s respectively. The upstream and middle stream have higher flow velocity than the downstream part, with an average flow velocity of 1.85m/s. The highest flow velocity of 2.67m/s occurs at the intersections of branches and the lowest at the entrance of the Hou Creek. Combined with related research(Zhang et al. 2015b; Zou et al. 2016b), the characteristics of flow velocity are associated with the terrain of the gully, with narrow and relatively steep channels in the intersections of the valley and the middle of the village, and wider and gentler channels in the downstream. The middle of the channel also has larger velocities than the edges at the same location of the valley, particularly pronounced in the gully channel at the middle of the village.

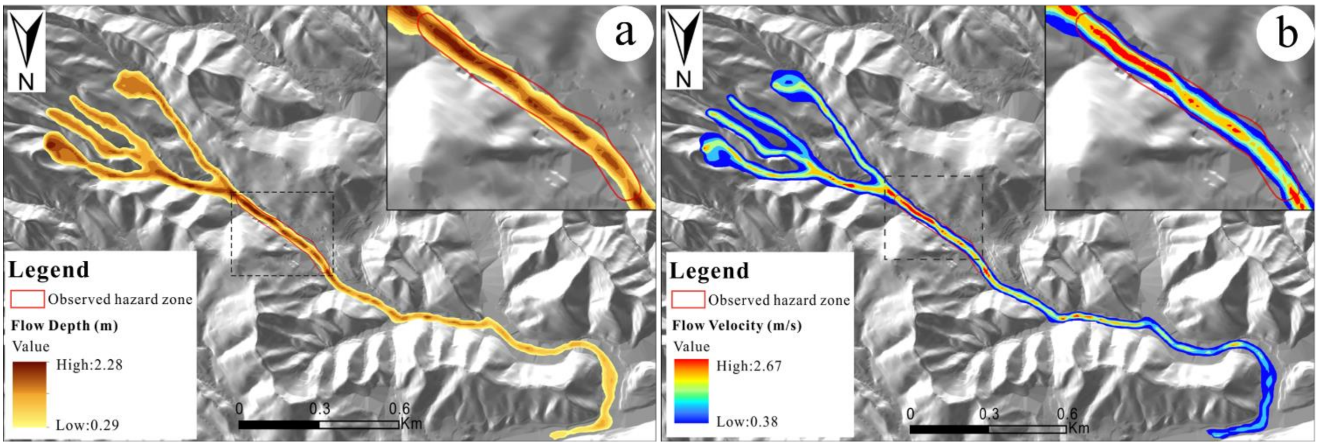

Figure 11 Reconstruction results of the WZW debris flow using FLO-2D model: (a) flow depth map, and (b) flow velocity map

4.3 Construction of vulnerability curves

The damge degree of buildings and the reconstruction results make it possible to assess the vulnerability of buildings using the vulnerability curve that relates the intensity of debris flow (flow depth and impact pressure) coupled with the damage degree of buildings (Tab.3). In this work, the impact pressure distribution of the 2019 WZW debris flow was calculated based the flow depth and flow velocity using Eq.12. Figure 12 exhibits the intensity results and the buildings damage degree distribution of the 2019 WZW debris flow. The buildings in extensive and complete damage degree mainly distributed in upstream of the village and concentrated in middle of the debris flow area, where the flow depth and impact pressure are higher.

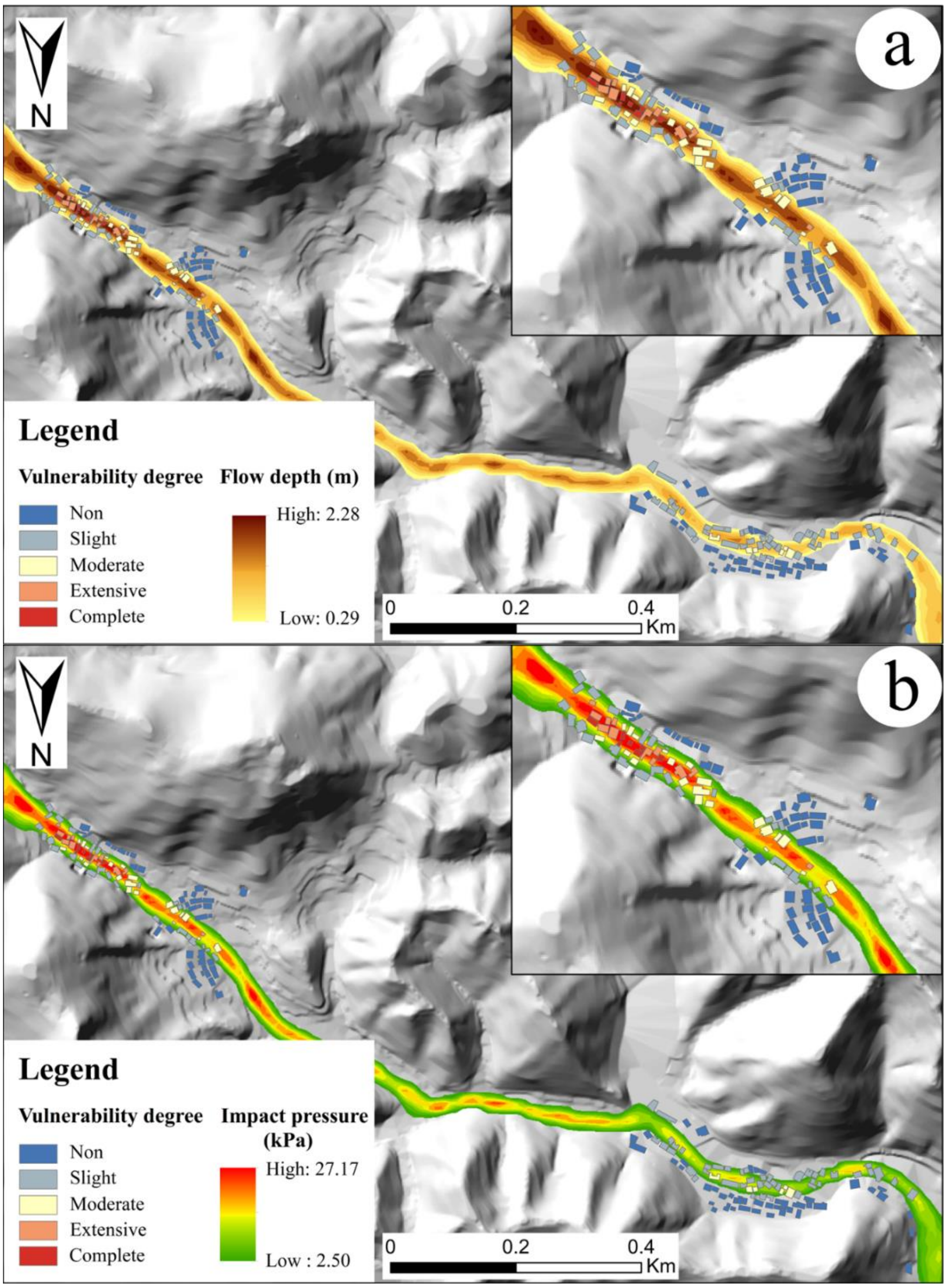

Figure 12 Intensity of the 2019 debris flow based on FLO-2D model and buildings distribution in different damage degrees: (a) flow depth distribution; (b) impact pressure distribution

The average vulnerability indexs of buildings in different damage degrees were used to develop the vulnerability curves. Figure 13 exhibits two empirical vulnerability curves which were functions of debris flow depth, debris flow impact pressure, respectively. Due to different resistance of non-RC frame and RC frame buildings to the debris flow, the structure of buildings were distinguished in the empirical vulnerability curves. The non-RC frame buildings exhibited a steeper increase in vulnerability curves with increasing flow depth and impact pressure than RC frame buildings. The intensity of debris flow required to cause extensive damage to an RC frame building can result in the complete destruction of Non-RC frame buildings. The difference in the vulnerability index between non-RC frame and RC frame buildings increases with the increasing of the intensity of debris flow. To achieve a vulnerability index of

1, a flow depth of 2.85 m and impact pressure of 37.3 kPa are required for non-RC frame buildings. In contract, for RC frame buildings, a flow depth of 5.32 m and impact pressure of 54.6 kPa are required.

An analytic expression was employed to establish the relationship between vulnerability and debris flow intensity. The selected function for the analysis was a sigmoid function with an “S” shape, which exhibits an asymptote from a value near zero to a finite value. Table 6 lists the vulnerability functions for the non-RC frame and RC frame buildings using the flow depth and impact pressure as the intensity indictors. The vulnerability functions make it possible to assessment the vulnerability index of buildings using debris flow intensity under different recurrence periods.

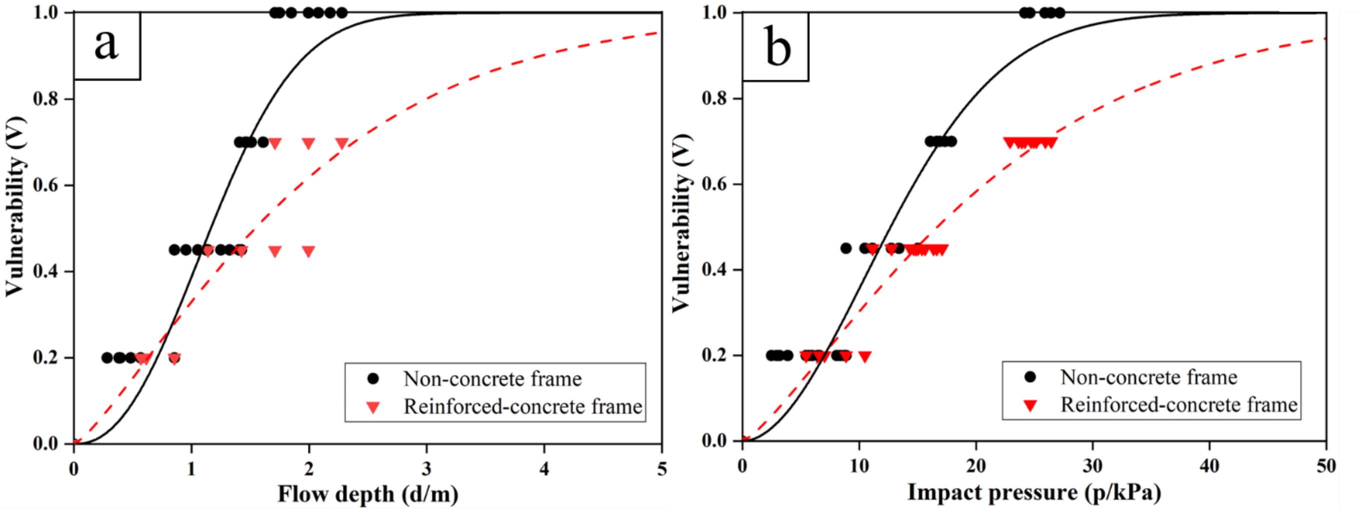

Figure 13 Debris flow vulnerability curves: (a) as a function of flow depth; (b) as a function of impact pressure

Table 6 Vulnerability functions for different type of building structures

Intensity parameter	Vulnerability function	
	Non-RC frame	RC frame
Flow depth [d (m)]	$V = 1 - e^{(-0.49 \times d^{2.28})}$	$V = 1 - e^{(-0.40 \times d^{1.27})}$
Impact pressure [p (kPa)]	$V = 1 - e^{(-0.44 \times (0.1 \times p)^{1.91})}$	$V = 1 - e^{(-0.36 \times (0.1 \times p)^{1.28})}$

4.4Intensity prediction of debris flows for different recurrence periods

Using the optimized rheological parameters from Section 4.1 and the flow hydrographs shown in Figure 5b, the FLO-2D software was also used to predict the movement and deposition of debris flow for the 50 and 100-year recurrence periods. Figure 14 displays the predicted flow depth, velocity and impact pressure maps of debris flows during 50 and 100-year recurrence periods. The results reveal that the highest flow velocity, flow depth and impact pressure are located around the intersections of branches and decrease as they move downstream. Additionally, the higher flow velocity, flow depth and impact pressure are concentrated in the middle of the channel. It's worth noting that high flow velocity tends to correspond to the maximum flow depth and flow velocity which may happened at different moments in the whole simulation process.

Simulation results for debris flow under different recurrence periods reveal variations in inundation area, flow depth, and flow velocity. As the recurrence period increases from 20 to 100 years, the inundation area increases. Specifically, under a 50-year recurrence period, the inundation area is 1.92×10^5 m^2, representing a 3.2% increase from the 20-year recurrence period. Under a 100-year recurrence period, the inundation area is $1.95 \times 10^5 m^2$, representing a 4.8% improvement from the 20-year recurrence period. The increased inundation areas are concentrated in the WZW village, indicating that more residents will be affected by debris flow under either 50 or 100-year recurrence periods. In the meantime, we can notice that the improvement of inundation area is limited with increasing of recurrence period, as the debris flow is also discharging into the river along with the development. Additionally, the flow depth also increases as recurrence period increases, with the maximum flow depth under a 100-year recurrence period being 25% higher than that under a 20-year recurrence period. Similarly, the maximum flow velocity under 100-year recurrence period is 32.6% higher than that under 20-year recurrence period. Combining the analysis results above, smaller occurrence probability of the debris flows usually means larger-scale inundation area with greater threat. Smaller-scale debris flows occur frequently but with smaller threat.

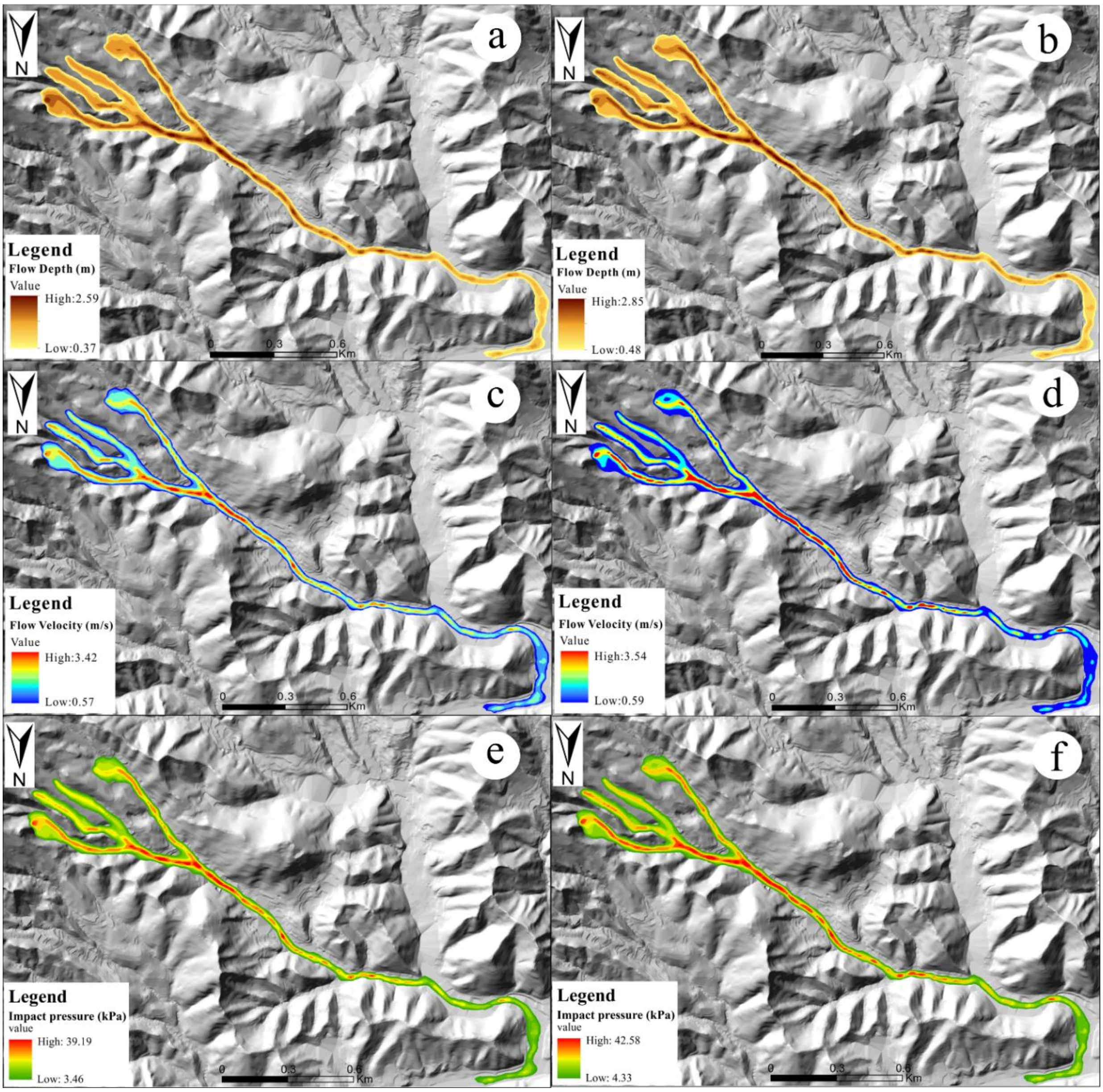

Figure 14 Predicted results of the WZW debris flow under different recurrence periods: (a) (b) flow depth maps for 50 and 100-year recurrence periods; (c) (d) flow velocity maps for 50 and 100-year recurrence periods; (e) (f) impact pressure maps for 50 and 100-year recurrence periods

4.5 Vulnerability assessment of the buildings

The vulnerability index of buildings under 50 and 100-year recurrence periods can be determined using the intensity indicators of debris flows (Fig.14) and vulnerability functions (Tab.6). Figure 15 shows the vulnerability maps for the 50 and 100-year recurrence periods. Under the 50-year recurrence period, 128 buildings are likely to be impacted. According to the vulnerability degree map using the flow depth as the intensity indictor (Fig.15a), 19 buildings would face the complete damage and 18 buildings would face extensive damage. While according to the vulnerability degree map using the impact pressure as the intensity indictor (Fig.15b), 30 buildings would suffer complete damage and 23 buildings would suffer extensive damage. The result above indicates that the vulnerability function using the impact pressure as the intensity indictor is more conservative than that using flow depth as the intensity indictor. The result exhibits the same pattern for the case of 100-year recurrence period. The vulnerability degree map using flow depth as the intensity indictor shows 23 buildings would face complete damage and 34 buildings would face extensive damage (Fig.15c). While 47 building would suffer complete damage and 22 buildings would suffer extensive damage according to the vulnerability degree map using impact pressure as the intensity indictor (Fig.15d).

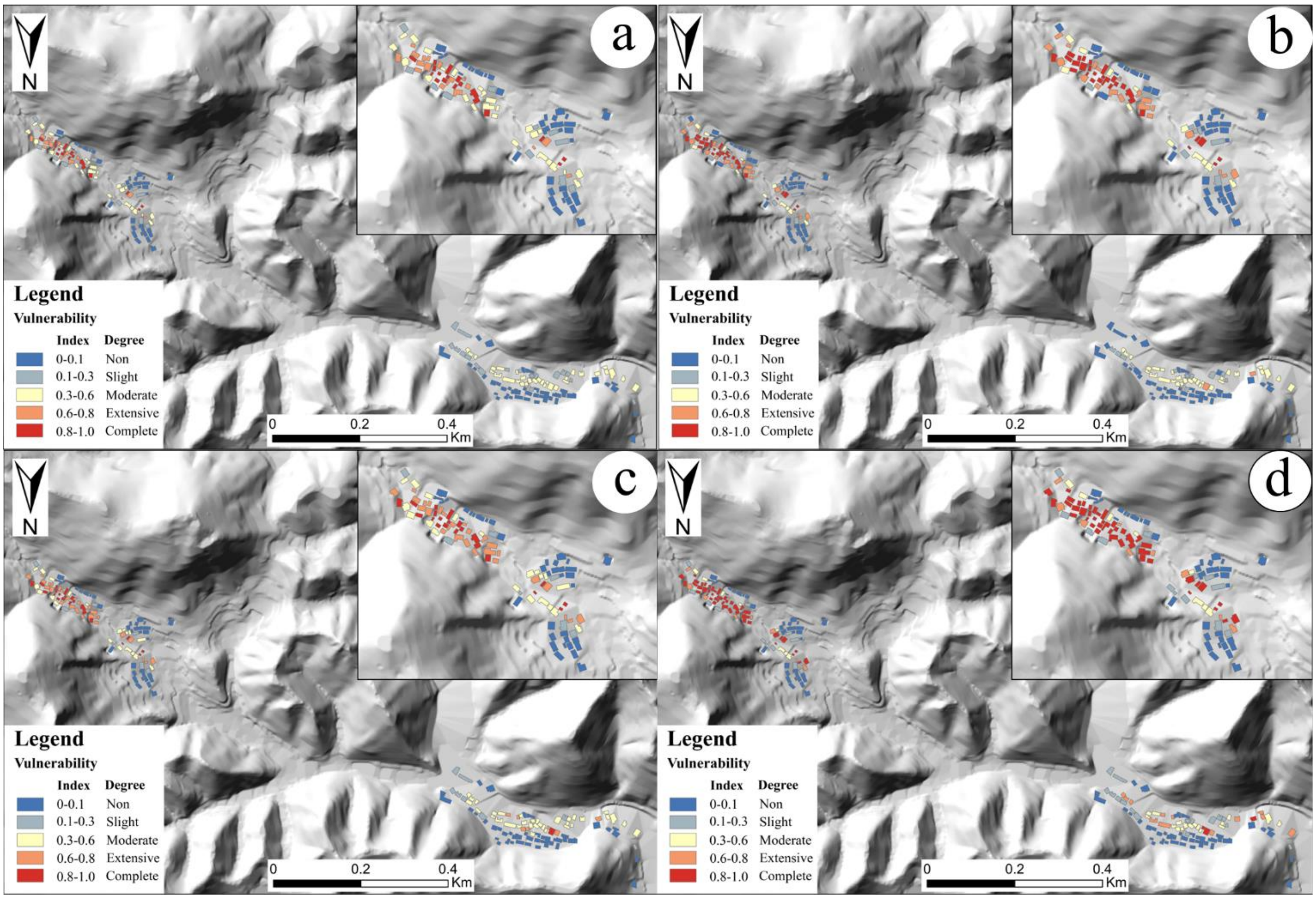

Figure 15 Building vulnerability maps under 50, 100-year recurrence periods: (a), (b) vulnerability for a 50-year recurrence period using the flow depth and impact pressure as the intensity indicator; (c), (d) vulnerability for a 100-year recurrence period using the flow depth and impact pressure as the intensity indicator

4.6 Quantitative risk assessment

The quantitative vulnerability result makes it possible to quantify the risk, particularly the direct economic loss to the buildings under different recurrence periods. According to Eq.11, the probability of a debris flow occurring ($P_{(L)}$) was assigned 0.02 and 0.01 for the 50 and 100-year recurrence period, respectively. Both the probability of a debris flow reaching a specific point ($P_{(T:L)}$) and the temporal-spatial probability of the elements ($P_{(S:T)}$) were set as 1. The vulnerability value of a specific building (V) was assigned based on the vulnerability index calculated in Section 4.5. The economic value of buildings (E) was calculated by multiplying the unit price by the total area of the building. According to the compensation standards for buildings with different structures for immigrants in Southeast China (Wei et al. 2021), the unit prices per square meter for buildings with RC frame structure and non-RC frame structure used in this study are ¥1720 and 1000/m^2, respectively. Figure 16 exhibits the annual debris flow risk maps under 50 and 100-year recurrence periods using two kinds of vulnerability functions. It's obvious that the annual risk of buildings is considerably affected by the difference of vulnerability functions. Risk reaches almost ¥ 10066/year for a single building in case of the flow depth vulnerability calculation and 12420/year for a single building in case of the impact pressure use.

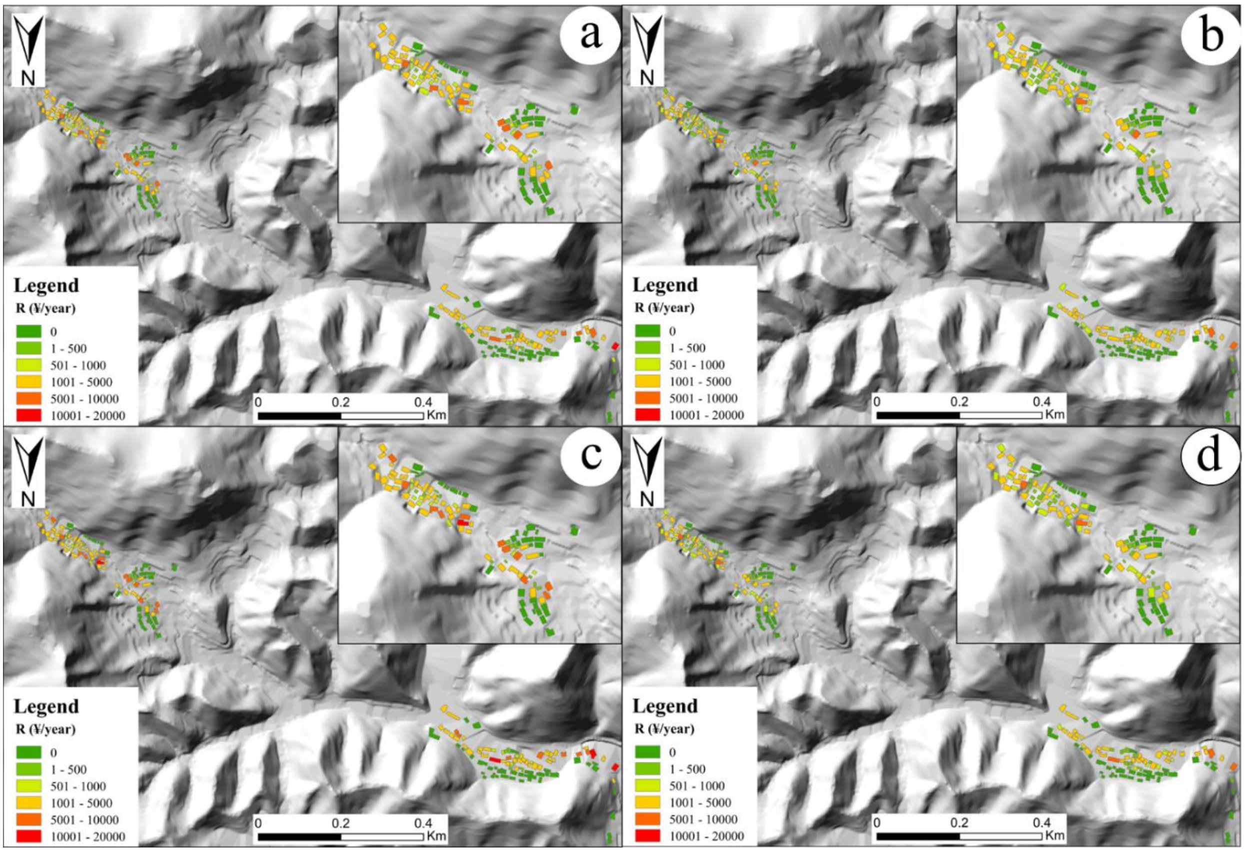

Figure 16 Debris flow annual risk map under a 50 and 100-year recurrence period: (a), (b) risk map for a 50-year recurrence period using the flow depth and impact pressure as the intensity indicator; (c), (d) risk map for a 100-year recurrence period using the flow depth and impact pressure as the intensity indicator

The annual economic risk and expected loss to all buildings in WZW village were calculated based on the annual risk map (Tab.7). Considering two kinds of vulnerability functions and the 50, 100-year recurrence period, the village would face a direct economic loss of ¥ 1.83-3.85 $\times$ 10^5/year. The expected loss would reach ¥ 1.56-1.93 $\times$ 10^7 when the debris flow occur under the condition of 50-year recurrence period, and the expected loss would reach ¥1.83-2.03 $\times$ 10^7 when the debris flows occur under the condition of 50-year recurrence period, respectively. The annual economic risk and expected loss to be faced could provide a sound foundation for local managers to implement risk management strategies and minimize human and economic losses.

Table 7 Overall risk to the WZW village under 50 and 100 year recurrence period

Recurrence period-intensity indicator	P(L)	P(T:L)	P(S:T)	V	E (¥/m2)	R (¥105/year)	Expected loss (¥107)
50Y-d	0.02	1	1		1720	3.12	1.56

50Y-p	0.02	1	1	0-1	(RC frame)	3.85	1.93
100Y-d	0.01	1	1		1000	1.83	1.83
100Y-p	0.01	1	1		(non-RC frame)	2.03	2.03

5. Discussion

In the simulation of debris flows, the factors that require attention may vary depending on the type of debris flow (Kim et al. 2018; Zhang et al. 2018). For debris flows on slopes, identifying the distribution and stability of landslides and collapses is crucial. While selecting the drainage point and determining the flow hydrograph are essential for channelized debris flows. The numerical simulation was used as an effective method of characterizing debris flows in this study, due to its precision and relatively low number of required parameters(Tang et al. 2011; Chen et al. 2012; Zou et al. 2016b). As sudden debris flows often lack continuous monitoring data, several methods have been developed to predict flow hydrographs (Chen et al. 2016; Chang et al. 2017; Wei et al. 2018). We chose a hydrological model, named SCS-CN model, for the watershed analysis. We used the SCS-CN model to perform a watershed analysis for generating the basin unit and the drainage point. On this basis, the flow hydrographs were determined based on the actual rainfall data and a digital elevation model (Fig.5b). The SCS-CN method has the advantage of incorporating real terrain data and being highly efficient, compared to the empirical formulae used in some previous studies (Zhang et al. 2015a; Wei et al. 2018).

The FLO-2D model was adopted in our study for the debris flow kinetic simulation. The initiation and features of debris flows can be characterized by this method, which enables the analysis of the risk in the study area. The accuracy of the modelled result depends on not only the quality of the input data, but also the rationality of rheological parameters(Ouyang et al. 2019; Chen et al. 2021). Firstly, the terrain data we adopted in this study was the digital elevation with high spatial resolution (2m) obtained from a photogrammetric survey using UAVs, which ensures the data is accurate and up-to-date. Secondly, we initially determined the range of rheological parameters by combining the debris flow features obtained from the field investigation and the recommended values in the FLO-2D manual. Then we used a series of validation procedures for the optimal selection of parameters. On one hand, we compared the reconstructed and observed influence areas to determine the overall accuracy of the simulated results, and performed trial-error selection and adjustments of the input rheological parameters. This approach has advantages in terms of accuracy and comprehensiveness comparing to other studies(Chen et al. 2021). Additionally, we placed monitoring points at the locations where mud marks were observed on buildings during field investigation and compared the predicted maximum depth and height of the mud marks. Through these two methods, the effectiveness of the hydrograph and runout models was verified. However, there are still some limitations in the validation process. The simulation result was validated from the aspect of inundation zone and flow depth, didn’t consider the flow velocity, as the lack of validated data about the flow velocity during the debris flow.

The vulnerability curves established in this study provided the possibility to quantify the vulnerability of buildings to the future debris flows in Typhoon-prone area. To justify the vulnerability curves, they have been compared with the related results(Barbolini et al. 2004; Quan Luna et al. 2011; Kang and Kim 2016). Figure 17 showed the comparison result of vulnerability curves based on the flow depth and impact pressure as the intensity indictors for the non-RC frame building. Barbolini et al. (2004) initially proposed a linear vulnerability curve only using the impact pressure as the intensity indictor based on the avalanche data in West Tyrol, Austria. Quan Luna et al. (2011) proposed two vulnerability curves based on the flow depth and impact pressure as the intensity indictor through numerical simulation and loss reports of Valtellina Valley, Northern Italy. The vulnerability curves built up by Kang et al. (2016) used the empirical formula and the buildings damage information of 11 debris flows. These four kinds of vulnerability curves show a good agreement in trend and range. For the flow depth vulnerability curves (Fig.17a), the vulnerability curve of this study located below that established by Kang et al. (2016), and above that established by Quan Luna et al. (2011). For the impact pressure vulnerability curves (Fig.17b), the vulnerability curve of this study located above others. In addition, we could notice that the vulnerability curves developed in this study more accurately represent the vulnerability index of buildings in this study area, which may relate to the differences in construction codes in different regions. The comparative results of the vulnerability curves in different study areas emphasized the uncertainty inherent in utilizing vulnerability function for quantitative risk assessment. The vulnerability curves proposed in our study have enriched the family of vulnerability curves for different type buildings, and have good applicability to other regions with similar debris flow hazards and built environments. And the method proposed in this study can be applied to quick construction of vulnerability curves for other building types in other specific study area.

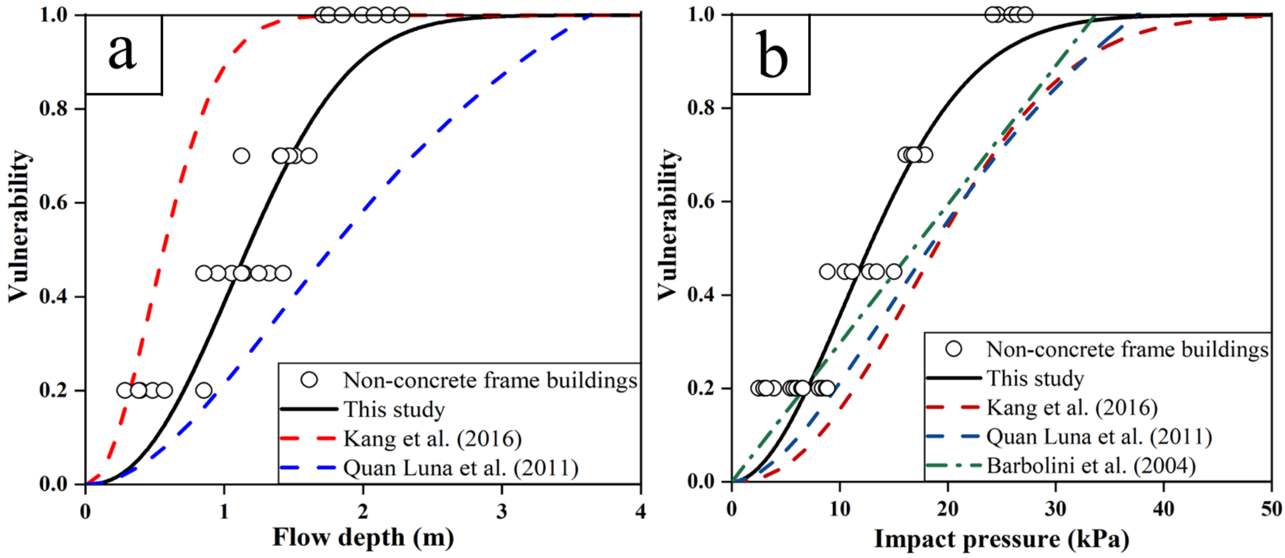

Figure 17 Comparison of the vulnerability curve calculated in this study and proposed by Kang et al. (2016), Quan Luna et al. (2011) and Barbolini et al. (2004) this research

To further compare the estimated vulnerability index using two kinds of vulnerability functions under the same recurrence period, figure 18 exhibits a scatter cloud of the vulnerability index of buildings to be affected. The fitted curves are approximately two straight lines going from 0 to 1 and the slopes of the curves are only 1.08, which demonstrated that two kinds of vulnerability results show a degree of consistency. The vulnerability function using the impact pressure as the indictor leads to slightly greater estimates than that using the flow depth as the indictor, and the percentage of extensive and extreme vulnerability degree is higher (Fig.15). The comparative results of the vulnerability index emphasized the uncertainty inherent in utilizing different intensity indictors for quantitative risk assessment. Comparing to relevant studies using other indicators, such as the product of flow depth and flow velocity(Tang et al. 1993), the product of flow velocity squared and flow depth(Chen et al. 2021), the impact pressure has clearer physical meaning which represents the damage ability of debris flow to buildings from the terms of hydrostatic pressure and dynamic overpressure. And the impact pressure has also widely used in other disaster risk assessment, for example the avalanches(Barbolini et al. 2004; Quan Luna et al. 2011).

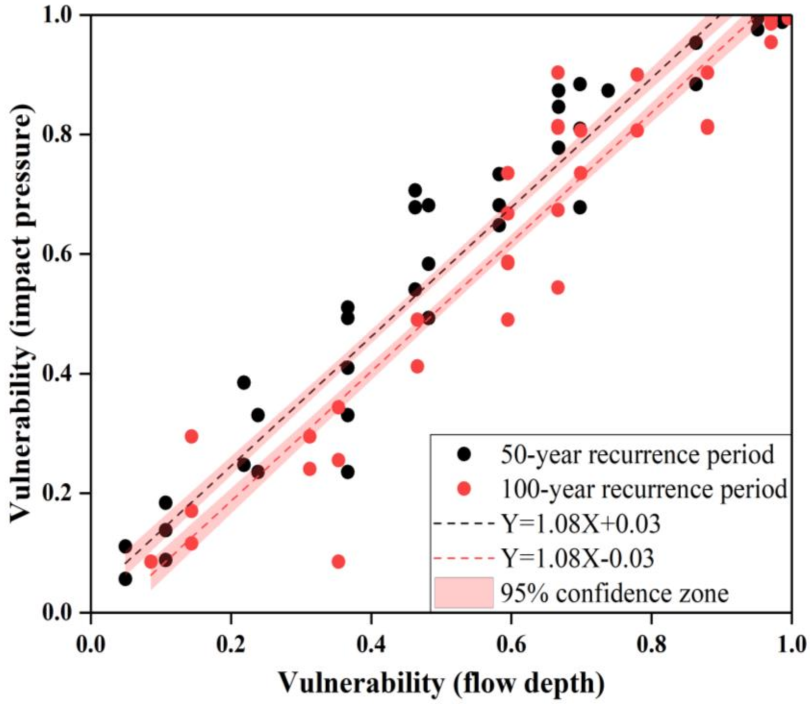

Figure 18 Scatter cloud of the vulnerability estimates for 50 and 100-year recurrence period using two vulnerability curves: the flow depth and impact pressure

This method adopted in this study abandoned the qualitative and semi-quantitative risk assessment, which exist many uncertainties and subjectivity. However, there are some certain limitations in the research process. First, during the modelling phase, we used a constant volume concentration (C_v) to represents the sediments entrainment capacity of the debris flow, without considering the change in topography and sediments volume. Second, under the condition of lacking research into the debris flow triggering mechanism, we used the recurrence period of rainfall to represent the recurrence period of debris flow occurrence. Third, the constructed vulnerability curves only consider the buildings structures, while other features also affect the resistance of buildings to debris flows such as buildings material, the number of floors. Last, our analysis of risk only focused on the economic risk of buildings, but the population and environmental risk are also important components of risk. These factors should be considered in future research to improve the comprehensiveness of risk assessment. These limitations highlight the need for further research in the future to improve the understanding and management of geohazard risks in urban areas.

6. Conclusion

This study attempted to quantitatively evaluate the risk of debris flows through building up the local vulnerability curves, which is crucial in helping local managers to manage the debris flow risk. The 2019 WZW debris flow was determined as a channelized flow caused by heavy rainfall and surface water runoff through a comprehensive survey method consisting of field investigations, remote sensing, and laboratory analysis. Shallow landslides and soil erosion resulted in a significant buildup of loose gravel and soil in the gully, providing the necessary material conditions. Additionally, the large vertical ratio of the channel and the confluence effect of the catchment area provided the necessary hydraulic and driving conditions for the formation of the debris flow. The typhoon-induced rainstorm with a daily intensity of 252.2 mm which had a recurrence period of 20 years, has surpassed the critical threshold of the debris flow occurrence.

The study presents a method to quantify the risk of debris flows in urban areas using a case study on the WZW gully. The features of the 2019 WZW debris flow were reconstructed using the SCS-CN model and FLO-2D model. Multiple validation process showed that the reconstruction results (inundation zone and flow depth) were consistent with the observed information. The accuracy evaluation parameter, ∂, reached 0.902, indicating the modelled results matches well with the actual situation.

We constructed different physical vulnerability curves for the RC frame building and non-RC frame building, based on the damage degree of buildings obtained from field investigation and the modelled debris flow intensity (flow depth and impact pressure). The debris flow intensity threshold of complete damage for the non-RC frame building corresponds to flow depth of 2.85m and impact pressure of 37.3kPa; The debris flow intensity threshold of complete damage for the RC frame building corresponds to flow depth of 5.32 m and impact pressure of 54.6 kPa. The uncertainty of quantitative risk assessment was considered in the building structure. The RC frame building has stronger resistance comparing to RC frame building. The vulnerability curve proposed in the study provided crucial basis to assess probability damage distribution of building in similar built environments for different debris flow intensity. The method proposed can be applied to quick construction of vulnerability curves for other building types in other specific study areas.

The potential intensities of future debris flow under 50 and 100-year recurrence periods were predicted based on the validated rheological parameters, considering different frequency of the triggering rainfall. Under a 50-year recurrence period, the maximum flow depth and flow velocity will reach 2.59 m and 3.42 m/s, and the maximum impact pressure will reach 39.19 kPa; Under the 100-year recurrence period, the maximum flow depth and flow velocity will reach 2.85m and 3.54 m/s, and the maximum impact pressure will reach 42.58 kPa. With the increasing of the recurrence period, the buildings in this study area will face the threat of debris flows with greater intensity.

The vulnerability index of every building under 50 and 100-year recurrence periods was calculated using the constructed vulnerability function based on the flow depth and impact pressure as the indictors. The vulnerability map based on the flow depth vulnerability function showed that there will be 18 and 30 buildings facing complete damage under 50 and 100-year recurrence periods respectively; The vulnerability map based on the impact pressure vulnerability function showed that there will be 23 and 40 buildings facing complete damage under 50 and 100-year recurrence periods respectively. The uncertainty of quantitative risk assessment was considered in the intensity indictor. The impact pressure vulnerability function is more conservative than the flow depth vulnerability function.

The annual risk of every building to be faced in the future was calculated based on the economic value and vulnerability index of buildings with different structures, consider 50 and 100-year recurrence periods. The annual economic risk and expected loss provided the practical value for local managers to make risk management strategies and land use planning.

Author Contributions

"Conceptualization, T.W. and Y.L.; methodology, T.W., K.Y; software, T.W.; investigation, T.W., Y.L.; data curation, C.X., L.C., and H.Z.; writing—original draft preparation, T.W.; writing—review and editing, K.Y., Y.L. and C.W.; visualization, T.W.; supervision, K.Y., C.W.; funding acquisition, L.C., K.Y. All authors have read and agreed to the published version of the manuscript.

Declaration of Competing Interest

The authors declare that there is no conflict of interests regarding the publication of this article.

Acknowledgments

This research was supported by the National Natural Science Foundation of China (No.41877525) and key research and development program of Hubei province (NO.2021BID009). The first author wishes to thank the China Scholarship Council (CSC) for funding his research period at University of Twente.

Reference

Barbolini M, Cappabianca F, Sailer R (2004) Empirical estimate of vulnerability relations for use in snow avalanche risk assessment. Risk Anal IV

Bout B, Lombardo L, van Westen CJ, Jetten VG (2018) Integration of two-phase solid fluid equations in a catchment model for flashfloods, debris flows and shallow slope failures. Environ Model Softw 105:1–16. https://doi.org/10.1016/j.envsoft.2018.03.017

Chang M, Liu Y, Zhou C, Che H (2020) Hazard assessment of a catastrophic mine waste debris flow of Hou Gully, Shimian, China. Eng Geol 275:105733. https://doi.org/10.1016/j.enggeo.2020.105733

Chang M, Tang C, Van Asch ThWJ, Cai F (2017) Hazard assessment of debris flows in the Wenchuan earthquake-stricken area, South West China. Landslides 14:1783–1792. https://doi.org/10.1007/s10346-017-0824-9

Chen H-X, Li J, Feng S-J, et al (2019) Simulation of interactions between debris flow and check dams on three-dimensional terrain. Eng Geol 251:48–62. https://doi.org/10.1016/j.enggeo.2019.02.001

Chen HX, Zhang LM, Chang DS, Zhang S (2012) Mechanisms and runout characteristics of the rainfall-triggered debris flow in Xiaojiagou in Sichuan Province, China. Nat Hazards 62:1037–1057. https://doi.org/10.1007/s11069-012-0133-5

Chen HX, Zhang S, Peng M, Zhang LM (2016) A physically-based multi-hazard risk assessment platform for regional rainfall-induced slope failures and debris flows. Eng Geol 203:15–29. https://doi.org/10.1016/j.enggeo.2015.12.009

Chen M, Tang C, Zhang X, et al (2021) Quantitative assessment of physical fragility of buildings to the debris flow on 20 August 2019 in the Cutou gully, Wenchuan, southwestern China. Eng Geol 293:106319. https://doi.org/10.1016/j.enggeo.2021.106319

Ciurean RL, Hussin H, van Westen CJ, et al (2017) Multi-scale debris flow vulnerability assessment and direct loss estimation of buildings in the Eastern Italian Alps. Nat Hazards 85:929–957. https://doi.org/10.1007/s11069-016-2612-6

Corominas J, van Westen C, Frattini P, et al (2013) Recommendations for the quantitative analysis of landslide risk. Bull Eng Geol Environ. https://doi.org/10.1007/s10064-013-0538-8

Cui P, Hu K, Zhuang J, et al (2011) Prediction of debris-flow danger area by combining hydrological and inundation simulation methods. J Mt Sci 8:1–9. https://doi.org/10.1007/s11629-011-2040-8

Eidsvig UMK, Papathoma-Köhle M, Du J, et al (2014) Quantification of model uncertainty in debris flow vulnerability assessment. Eng Geol 181:15–26. https://doi.org/10.1016/j.enggeo.2014.08.006

Fangqiang W, Yu Z, Kaiheng H, Kechang G (2006) Model and method of debris flow risk zoning based on momentum analysis. Wuhan Univ J Nat Sci 11:835–839. https://doi.org/10.1007/BF02830173

Fell R, Corominas J, Bonnard C, et al (2008) Guidelines for landslide susceptibility, hazard and risk zoning for land-use planning. Eng Geol 102:99–111. https://doi.org/10.1016/j.enggeo.2008.03.014

Figueroa-García JE, Franco-Ramos O, Bodoque JM, et al (2021) Long-term lahar reconstruction in Jamapa Gorge, Pico de Orizaba (Mexico) based on botanical evidence and numerical modelling. Landslides 18:3381–3392. https://doi.org/10.1007/s10346-021-01716-3

Fuchs S, Heiss K, Hübl J (2007) Towards an empirical vulnerability function for use in debris flow risk assessment. Nat Hazards Earth Syst Sci 7:495–506. https://doi.org/10.5194/nhess-7-495-2007

Guo ZZ, Chen LX, Gui L, et al (2020) Landslide displacement prediction based on variational mode decomposition and WA-GWO-BP model. Landslides 17:567–583. https://doi.org/10.1007/s10346-019-01314-4

He K, Liu B, Hu X, et al (2022) Rapid Characterization of Landslide-Debris Flow Chains of Geologic Hazards Using Multi-method Investigation: Case Study of the Tiejiangwan LDC. Rock Mech Rock Eng 55:5183–5208. https://doi.org/10.1007/s00603-022-02905-9

HEC-HMS (2010) Hydrologic Modeling System. US Army Corps of Engineers, Hydrologic Engineering Center (HEC) Davis

Horton AJ, Hales TC, Ouyang C, Fan X (2019) Identifying post-earthquake debris flow hazard using Massflow. Eng Geol 258:105134. https://doi.org/10.1016/j.enggeo.2019.05.011

Hu KH, Ding MT (2012) Hazard mapping for debris flows based on numerical simulation and momentum index. 2nd Int Conf Proc Mt Environ Dev 27–34

Jaiswal P, van Westen CJ (2013) Use of quantitative landslide hazard and risk information for local disaster risk reduction along a transportation corridor: a case study from Nilgiri district, India. Nat Hazards 65:887–913. https://doi.org/10.1007/s11069-012-0404-1

Jakob M, Stein D, Ulmi M (2012) Vulnerability of buildings to debris flow impact. Nat Hazards 60:241–261.

https://doi.org/10.1007/s11069-011-0007-2

Kang H, Kim Y (2016) The physical vulnerability of different types of building structure to debris flow events. Nat Hazards 80:1475–1493. https://doi.org/10.1007/s11069-015-2032-z

Kim M-I, Kwak J-H, Kim B-S (2018) Assessment of dynamic impact force of debris flow in mountain torrent based on characteristics of debris flow. Environ Earth Sci 77:538. https://doi.org/10.1007/s12665-018-7707-9

Laouacheria F, Mansouri R (2015) Comparison of WBNM and HEC-HMS for Runoff Hydrograph Prediction in a Small Urban Catchment. Water Resour Manag 29:2485–2501. https://doi.org/10.1007/s11269-015-0953-7

Li Z, Nadim F, Huang H, et al (2010) Quantitative vulnerability estimation for scenario-based landslide hazards. Landslides 7:125–134. https://doi.org/10.1007/s10346-009-0190-3

Liang X, Segoni S, Yin K, et al (2022) Characteristics of landslides and debris flows triggered by extreme rainfall in Daoshi Town during the 2019 Typhoon Lekima, Zhejiang Province, China. Landslides 19:1735–1749. https://doi.org/10.1007/s10346-022-01889-5

Liu X, Lei J (2003) A method for assessing regional debris flow risk: an application in Zhaotong of Yunnan province (SW China). Geomorphology 52:181–191. https://doi.org/10.1016/S0169-555X(02)00242-8

Luna BQ, Remaître A, van Asch ThWJ, et al (2012) Analysis of debris flow behavior with a one dimensional run-out model incorporating entrainment. Eng Geol 128:63–75. https://doi.org/10.1016/j.enggeo.2011.04.007

Matti B, Dahlke HE, Lyon SW (2016) On the variability of cold region flooding. J Hydrol 534:669–679. https://doi.org/10.1016/j.jhydrol.2016.01.055

Nie J, Zhang X, Xu C, et al (2021) The impact of super typhoon lekima on the house collapse rate and quantification of the interactive impacts of natural and socioeconomic factors. Geomat Nat Hazards Risk 12:1386–1401. https://doi.org/10.1080/19475705.2021.1927860

O'Brien JS, Julien PY, Fullerton WT (1993) Two-Dimensional Water Flood and Mudflow Simulation. J Hydraul Eng 119:244–261. https://doi.org/10.1061/(ASCE)0733-9429(1993)119:2(244)

Ouyang C, Wang Z, An H, et al (2019) An example of a hazard and risk assessment for debris flows—A case study of Niwan Gully, Wudu, China. Eng Geol 263:105351. https://doi.org/10.1016/j.enggeo.2019.105351

Papathoma-Köhle M, Keiler M, Totschnig R, Glade T (2012) Improvement of vulnerability curves using data from extreme events: debris flow event in South Tyrol. Nat Hazards 64:2083–2105. https://doi.org/10.1007/s11069-012-0105-9

Peduto D, Ferlisi S, Nicodemo G, et al (2017) Empirical fragility and vulnerability curves for buildings exposed to slow-moving landslides at medium and large scales. Landslides 14:1993–2007. https://doi.org/10.1007/s10346-017-0826-7

Quan Luna B, Blahut J, Camera C, et al (2013) Physically based dynamic run-out modelling for quantitative debris flow risk assessment: a case study in Tresenda, northern Italy. Environ Earth Sci. https://doi.org/10.1007/s12665-013-2986-7

Quan Luna B, Blahut J, van Westen CJ, et al (2011) The application of numerical debris flow modelling for the generation of physical vulnerability curves. Nat Hazards Earth Syst Sci 11:2047–2060. https://doi.org/10.5194/nhess-11-2047-2011

Scheidl C, Rickenmann D (2009) Empirical prediction of debris-flow mobility and deposition on fans. Earth Surf Process Landf n/a-n/a. https://doi.org/10.1002/esp.1897

Tang C, Liu X, Zhu J (1993) The evaluation and application of risk degree for debris flow inundation on alluvial fans. J Nat Disasters 2:79–84

Tang C, Zhu J, Ding J, et al (2011) Catastrophic debris flows triggered by a 14 August 2010 rainfall at the epicenter of the Wenchuan earthquake. Landslides 8:485–497. https://doi.org/10.1007/s10346-011-0269-5

Tang C, Zhu J, Li WL, Liang JT (2009) Rainfall-triggered debris flows following the Wenchuan earthquake. Bull Eng Geol Environ 68:187–194. https://doi.org/10.1007/s10064-009-0201-6

Tang Y, Guo Z, Wu L, et al (2022) Assessing Debris Flow Risk at a Catchment Scale for an Economic Decision Based on the LiDAR DEM and Numerical Simulation. Front Earth Sci 10:821735. https://doi.org/10.3389/feart.2022.821735

van Asch ThWJ, Tang C, Alkema D, et al (2014) An integrated model to assess critical rainfall thresholds for run-out distances of debris flows. Nat Hazards 70:299–311. https://doi.org/10.1007/s11069-013-0810-z

Wei L, Hu K, Liu J (2021) Quantitative Analysis of the Debris Flow Societal Risk to People Inside Buildings at Different Times: A Case Study of Luomo Village, Sichuan, Southwest China. Front Earth Sci 8:627070. https://doi.org/10.3389/feart.2020.627070

Wei Z, Xu Y-P, Sun H, et al (2018) Predicting the occurrence of channelized debris flow by an integrated cascading model: A case study of a small debris flow-prone catchment in Zhejiang Province, China. Geomorphology 308:78–90. https://doi.org/10.1016/j.geomorph.2018.01.027

Yu B, Ma Y, Wu Y (2013) Case study of a giant debris flow in the Wenjia Gully, Sichuan Province, China. Nat Hazards 65:835–849. https://doi.org/10.1007/s11069-012-0395-y

Zanchetta G, Sulpizio R, Pareschi MT, et al (2004) Characteristics of May 5–6, 1998 volcaniclastic debris flows in the Sarno area (Campania, southern Italy): relationships to structural damage and hazard zonation. J Volcanol Geotherm Res 133:377–393. https://doi.org/10.1016/S0377-0273(03)00409-8

Zhang P, Ma J, Shu H, et al (2015a) Simulating debris flow deposition using a two-dimensional finite model and Soil Conservation Service-curve number approach for Hanlin gully of southern Gansu (China). Environ Earth Sci 73:6417–6426. https://doi.org/10.1007/s12665-014-3865-6

Zhang P, Ma J, Shu H, et al (2015b) Simulating debris flow deposition using a two-dimensional finite model and Soil Conservation Service-curve number approach for Hanlin gully of southern Gansu (China). Environ Earth Sci 73:6417–6426. https://doi.org/10.1007/s12665-014-3865-6

Zhang S, Zhang L, Li X, Xu Q (2018) Physical vulnerability models for assessing building damage by debris flows. Eng Geol 247:145–158. https://doi.org/10.1016/j.enggeo.2018.10.017

Zhang X, Chen G, Cai L, et al (2021) Impact Assessments of Typhoon Lekima on Forest Damages in Subtropical China Using Machine Learning Methods and Landsat 8 OLI Imagery. Sustainability 13:4893. https://doi.org/10.3390/su13094893

Zhao H, Duan X, Raga GB, Klotzbach PJ (2018) Changes in Characteristics of Rapidly Intensifying Western North Pacific Tropical Cyclones Related to Climate Regime Shifts. J Clim 31:8163–8179. https://doi.org/10.1175/JCLI-D-18-0029.1

Zhou C, Chen P, Yang S, et al (2022) The impact of Typhoon Lekima (2019) on East China: a postevent survey in Wenzhou City and Taizhou City. Front Earth Sci 16:109–120. https://doi.org/10.1007/s11707-020-0856-7

Zou Q, Cui P, Zeng C, et al (2016a) Dynamic process-based risk assessment of debris flow on a local scale. Phys Geogr 37:132–152. https://doi.org/10.1080/02723646.2016.1169477

Zou Q, Cui P, Zeng C, et al (2016b) Dynamic process-based risk assessment of debris flow on a local scale. Phys Geogr 37:132–152. https://doi.org/10.1080/02723646.2016.1169477